Thiazolidine ring-opening and deprotonation. Computational DFT study

Kuvek, Tea

Master's thesis / Diplomski rad

2022

Degree Grantor / Ustanova koja je dodijelila akademski / stručni stupanj: **University of Zagreb, Faculty of Pharmacy and Biochemistry / Sveučilište u Zagrebu, Farmaceutsko-biokemijski fakultet**

Permanent link / Trajna poveznica: https://urn.nsk.hr/urn:nbn:hr:163:568371

Rights / Prava: In copyright/Zaštićeno autorskim pravom.

Download date / Datum preuzimanja: **2024-05-02**

Tea Kuvek

Thiazolidine ring-opening and deprotonation. Computational DFT study.

DIPLOMA THESIS

Submitted to University of Zagreb Faculty of Pharmacy and Biochemistry

Zagreb, 2021.

TABLE OF CONTENTS

1.   INTRODUCTION

1.1   Pharmaceuticals in aquatic environment and soil

Pharmaceuticals are compounds used as medicinal drugs to cure or prevent a disease in either humans or animals. Rapid economic development and better living conditions led to longer life expectancy, which increased the total population, in particular the elderly group. This may result with increased demand of pharmaceuticals for people in domestic use or in hospitals, followed by increased pharmaceutical waste (Li, 2014). Pharmaceuticals belong to the group of so-called "new pollutants", together with the products used to improve quality of everyday life such as moisturizers, lipsticks, shampoos, hair dyes, deodorants and toothpastes. Their concentration in the environment poses a potential hazard to the ecosystem due to non-existent regulation on their environmental release. A special environmental problem are also pharmaceuticals' degradation products and metabolites, moreover because they are not scientifically examined in most of the cases (Hok, 2017). "New pollutants" get into environment through landfills, animal waste, freshwater aquaculture waste, hospital waste, industrial waste or domestic waste (Figure 1).

Unfortunately, environmental pollution by pharmaceuticals is not the only problem that the deposition of these compounds entails. Pharmaceutical waste can cause detrimental effects to the health of animals and plants, including renal failure, impaired reproduction, and inhibition of growth of certain aquatic species. For example, fish have been particularly affected by waste discharge into waterways; it was recorded that male fishes in Europe's rivers are inter-sex, displaying both male and female sexual characteristics due to presence of estrogen-mimicking substances (De Metrio *et al.*, 2003). Antimicrobial resistance has been considered one of the major threats to public health by World Health Organization (WHO) and is expected to cause 10 million deaths per year in 2050. Pharmaceutical waste disposal is one of the factors contributing to this problem that has devastating impacts on people and animals coming into contact with highly resistant bacteria. Because of all the reasons above and many more, it is urgent to find a sustainable solution for pharmaceuticals disposal.
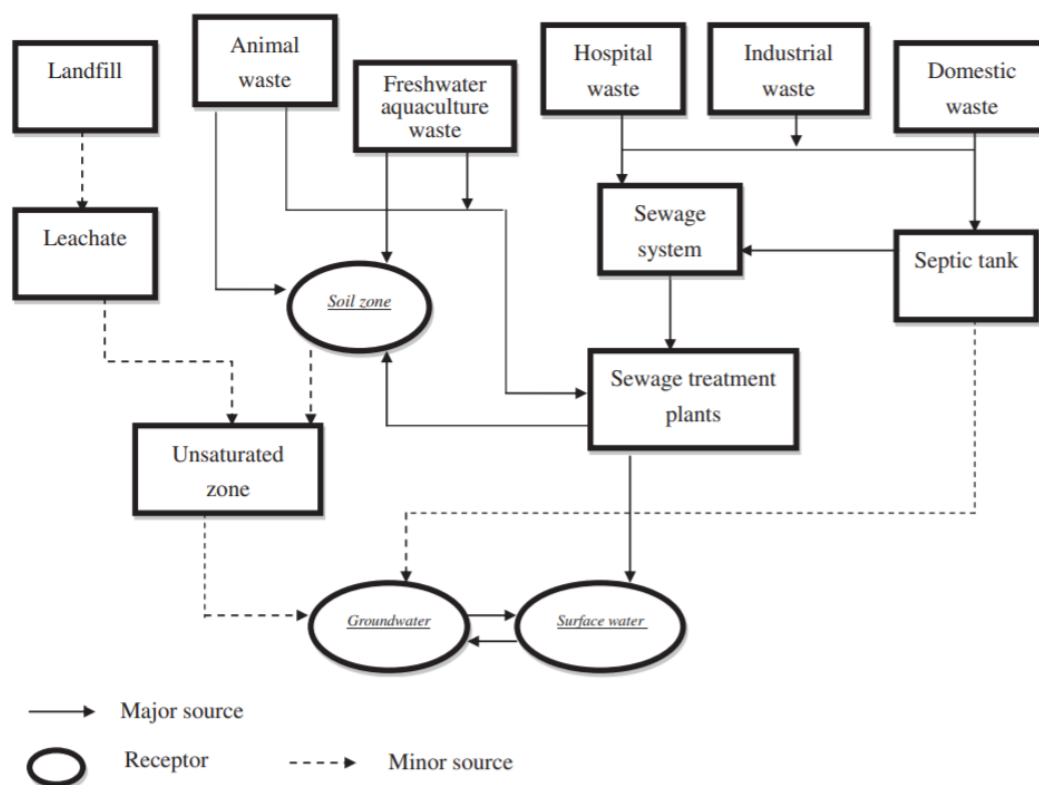
Figure 1. Potential sources and pathways of pharmaceuticals pollution in soil and water (Li, 2014).

1.2   Penicillins

Penicillins are a group of molecules originally obtained from *Penicillium* moulds and are members of β-lactam antibiotics. Since their discovery, they became widely used for treatment of wide spectra of bacterial infections. Penicillins are still frequently used today, though many types of bacteria have developed resistance following extensive use in the past decades. The key structural feature of penicillins is the four-membered β-lactam ring, as it shows penicillin's antibacterial activity. The β-lactam ring itself is fused to a five-membered thiazolidine ring, while it has amide side chain present on the other side (Figure 2).
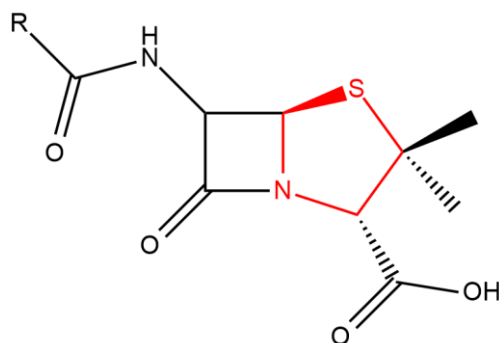
Figure 2. Penicillin structure with thiazolidine ring painted in red.

As well as the mentioned pharmaceuticals, among which are antibiotics, penicillins are ubiquitous in the environment. Since these are the longest-used antibiotics, bacterial resistance towards them has been observed to a greater extent than in others. Many papers indicate that penicillin drug in water and soil is the main cause of this phenomenon (Wang *et al.*, 2020). Another example of environmental damage caused by penicillins, and antibiotics in general, is the alteration of microbial diversity leading to the extinction of species of flora and fauna (Bengtsson-Palme *et al.*, 2019).

1.3 Thiazolidine

Thiazolidine is a heterocyclic organic compound shown in red colour in Figure 2. It is a 5-membered saturated ring with a thioether group in the position 1 and an amine group in the position 3. As a well-known molecule whose derivatives have been used for various purposes, it has chemical and physical properties firmly defined. The presence of sulphur enhances thiazolidines' pharmacological properties, and, therefore, they are used as vehicles in the synthesis of valuable organic combinations. They show varied biological properties such as: anticancer, anticonvulsant, antimicrobial, anti-inflammatory, neuroprotective, antioxidant activity and so on. This diversity in the biological response makes it a highly prized moiety (Sahiba *et al.*, 2020). Apart from penicillins, which are the best known compounds with thiazolidine ring in their structure, there is a broad list of registered drugs that share this structural part, e.g. diabetes mellitus type 2 drugs, diuretics and anticonvulsants (Figure 3).
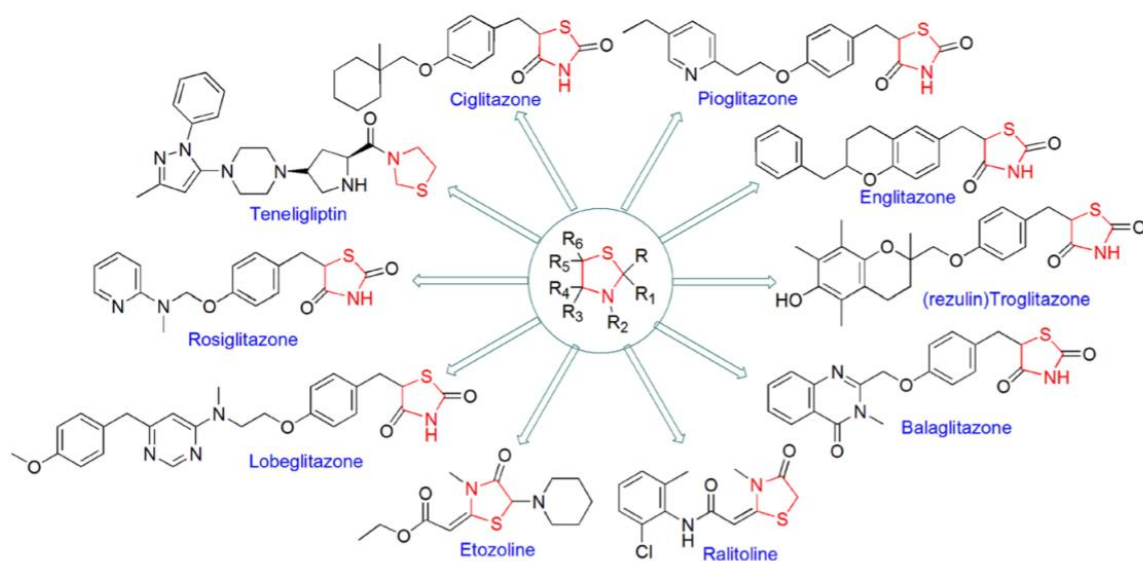
Figure 3. Available thiazolidine-based drugs (Sahiba *et al.*, 2020).

1.3.1 Thiazolidine ring-opening reaction

Since thiazolidine and its derivatives are well-known and long-studied molecules, many of the chemical reactions in which they participate have been reported and characterized. One of these is the opening of the thiazolidine ring, during which the C-S bond breaks. So far, it has been commonly described as alkaline (Davis *et al.,* 1991) or pH-independent hydrolysis (Fife *et al.*, 1991). It is also known, in the lab where this research took place, that UV light can induce ring-opening of thiazolidine and examined derivatives, but such process is far to be understood and therefore needs further consideration. In order to fully understand and describe the process of ring opening, one has to use the computational methods to elucidate the experimentally observed phenomenon.

2.   OBJECTIVES

The aim of this thesis is to investigate by quantum-chemical calculations the experimentaly observed thiazolidine ring opening driven by UV light. Since the reaction is very fast and the products unstable, it was necessary to study the process using computational chemistry to gather a deeper understanding. The main objective of this work is the calculation of acidity constants, chemical equilibrium constants (especially for the ring-opening reaction), global reactivity descriptors, UV-Vis absorption maxima and one-electron reduction potentials of thiazolidine, 2-methyl-thiazolidine, 2-(4'-hydroxy)-phenyl-thiazolidine and N-methyl-thiazolidine. All calculated values provide insight into the chemistry of the experimentally observed reaction, which has not been reported so far in the literature. In the future, this could be a useful and affordable tool for studying degradation of penicillin antibiotics and molecules containing the thiazolidine moiety present in wastewater.

3. MATERIALS AND METHODS

3.1 Computational chemistry

Computational chemistry is a branch of chemistry that uses mathematical approximations incorporated in computer programmes to calculate various molecular properties such as total energy, dipole moment, reactivity, frequency vibrations and more. Since it is less time-consuming, more affordable and ecologically safer comparing to actual experiments, scientists begin their research using computational methods to make predictions and gather information about molecules of interest. It is also widely used for better understanding and analysis of experimentally gleaned data, as well as for characterizing molecules impossible to isolate. Almost every aspect of chemistry can be described in a qualitative or approximate quantitative computational scheme, but very few aspects can be computed exactly.

3.2 Model chemistry

Model chemistry is a technique that includes all theoretical and computational methods to describe the nature of a certain molecule. Depending on whether they include empirical or experimental data, methods in chemistry modelling can be divided into three main categories:

a) *ab initio* (Latin for "from scratch") - uses empirical data only
b) semi-empirical - uses both empirical and experimental data
c) molecular mechanics - uses experimental data only.

Important characteristics that distinguish one category from another are level of simplification, generality (possibility to use for general or only specific problems), limitations (range of applicability and accuracy), cost and efficiency. Each model has its advantages and disadvantages for a particular use, so it is necessary to choose the optimal one.

3.3 Quantum-chemical methods

Quantum-chemical methods include mentioned *ab initio* and semi-empirical, but also DFT (*Density Functional Theory*) methods. They are based on solving the Schrödinger equation, equation that can be solved accurately for one electron systems only. Therefore, for calculating properties of a real system, approximations are used and differ from method to method.

Semi-empirical methods use experimentally obtained parameters to estimate the change in geometry which results in lowest possible energy of the system. The advantage of these methods is their speed, but they can't deliver sufficient electronic interactions description. The problem is also variability, which originates from the difference between the system from which the experimental data are gathered and the observed one.

Ab initio methods, on the other hand, give consistent results of exceptional precision. This is understandable given the fact that these methods split the Schrödinger equation for several electrons chemical species into many one-electron equations that describe each electron in the field of others surrounding it. These methods are divided into Hartree-Fock method, which ignores electronic correlation, and post-Hartree-Fock method, which takes it into account. Unlike semi-empirical methods, the disadvantage of *ab initio* ones is long duration and high memory usage.

In this research DFT methods were used. They are based on Kohn-Sham theorem which correlates ground state energy of the system with electronic density of the molecule. By their characteristics, DFT methods can be compared with both *ab initio* and semi-empirical ones. With *ab initio* methods they share iterative calculation procedure, *i.e.* the behaviour of each electron in relation to the electron density of the system is described. However, the exact functional that connects electronic density with energy is not yet described, so it is necessary to include some experimental parameters. This is what DFT and semi-empirical methods have in common. DFT methods are the most frequently used ones, mainly for their precision, consistency, less time consuming and low memory usage, which means they take the best from both *ab initio* and semi-empirical methods. (Šakić, 2015)

DFT functionals differ from one another depending on definition of exchange functional, correlation functional, and share of HF functional as an edition to the exchange one. The most common method used is B3LYP (Becke, 3-parameter, LEE-Yang-Parr), which consist of Becke exchange functional (B), correlation functional developed by Lee, Yang and Parr (LYP) and a certain share of HF functional (20%). It belongs to BLYP functionals family and represents a hybrid of BLYP method (which has 0% of Hartree-Fock exchange) (Becke, 1988).

There are also, so-called, composite methods, which consist of different DFT methods combined. Composite methods have been developed with the aim of reaching chemical accuracy in larger systems. One of such methods used in this work is the CBS-QB3 that belongs to the family of the Complete Basis Set (CBS) methods of Petersson and co-workers (Sirjean *et al.*, 1999).

3.4 Basis sets

In theoretical and computational chemistry, basis sets represent a wave function with finite number of basis functions. The larger number of basis functions gives the better molecular orbital description (Foresman and Frisch, 1996). Basis sets are necessary to transform partial differential equations into algebraic equations, which are then applicable in computer programmes.

Basis sets can be composed of atomic orbitals (common choice in quantum chemistry), plane waves (usually applied for solid state analysis) or real-space approaches. There are three types of atomic orbitals used: natural atomic orbitals, Slater-type orbitals and Gaussian-type orbitals. The latter are the most frequently used ones, and they differ from one another in depending of two criteria: first is the number of primitive Gaussian functions which define inner orbitals or from which the functions that describe valence orbitals are composed of, and the second is whether there are polarization or diffusion functions involved.

Two basis sets were used for the purposes of this research: 6-31G(d,p) and 6-311++G(d,p).

The dash separates the core (on the left) from valence (on the right) orbital description. Six, in both basis sets, stands for the number of primitive Gaussian functions which describe inner orbitals, while the valence ones are split into two or three basis functions respectively.

Non hydrogen atoms have the addition of one set of d functions and hydrogen atoms have the addition of one set of p functions, which is represented by (d,p). In 6-311++G(d,p) basis set, the "++" notation stands for the addition of a set of diffuse s functions to hydrogen together with the addition of a set of diffuse sp orbitals to the atoms in the first and second rows.

3.5 Geometry optimization

To make sure that molecule is in its conformation of minimum energy, it is necessary to optimize the proposed structure. Geometry optimization is an iterative procedure that, by the means of optimization algorithms, within a certain coordinate system which defines position of all nuclei of the molecule, determinates the molecular structure at the minimum of electronic energy. This calculation leads to small structural changes of the molecule (bond length, bond and dihedral angles); each calculated conformation has different energy value and is associated to one point on the potential energy surface (PES) (Figure 4). PES, therefore, shows how the energy of molecule varies depending on the structural change (Foresman and Frisch, 1996). Geometry optimization locates stationary points on PES, where the first derivative of the energy

with respect to the change of atomic coordinates equals zero. The stationary point in which moving to either side on PES results in energy rise is a potential minimum (placed in a potential well on PES). A potential maximum, on the other hand, is referred to as either a transition state (TS) –strictly speaking a transition structure- or a saddle point, and it connects two local minima. To define whether the localised stationary point is minimum or TS, additional analysis is required (Hok, 2017).
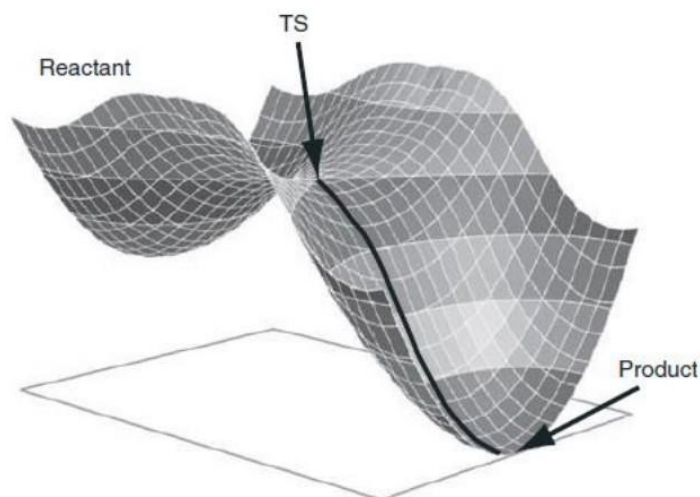
Figure 4. Potential energy surface scheme. The dark line represents a chemical reaction from reactant to product through transition state (TS), which connects two local minima (Bachrach, 2014).

Geometry optimization begins with the calculation of the energy and energy gradient of the proposed structure with arranged position of atoms in the molecule and the position of the molecule in the coordinate system. The change in geometry for the next optimization step is determined by the change in force and energy in different directions.

After each iteration, the system displays the status of the optimization calculation. In order to correctly determine the stationary point, *i.e.* to determine if the forces are very close to zero, the convergence criteria that the system must meet are given. They include information on the remaining maximum force on a particular atom in the molecular system, the average force on all atoms, the maximum structural change of a particular coordinate, and the average change of all structural parameters in the last two iterations (Filipović, 2018).

3.6   Frequency calculations

As mentioned earlier, to fully characterize the stationary point additional work is required. With this aim, but also to determinate force constants, frequency motion of atoms within molecules, thermodynamic data and to predict IR and Raman spectra, frequency calculations are performed. By solving the vibrational Schrödinger equation and calculating second energy derivatives with respect to nuclear coordinates, frequency calculation determines the frequency of the normal modes of vibrations. Therefore, together with the knowledge of molecular vibrations, these calculations answer the question whether the located stationary point is a transition structure (TS) –commonly also reported as a transition state– or a minimum. If there is only one imaginary vibrational frequency, stationary point is a minimum in all directions but in the one of that imaginary frequency and that structure represents a TS for the chemical reaction on the PES. When there are no imaginary frequencies, the analysed structure corresponds to minimum.

3.7   Intrinsic reaction coordinate (IRC)

Once the structure is characterised as TS, the local minima that connects the TS needs to be found. The computational technique used to find the minimum energy reaction pathway is the intrinsic reaction coordinate (IRC) (Fukui, 1981). The starting point of this calculation is the TS structure, which is then optimized in two directions: towards reactants and to products. The resulting minima correspond to reactants and products.

3.8   Time-dependant density functional theory (TD-DFT)

Time-dependant density functional theory (TD-DFT) is a quantum-mechanical theory used in physics and chemistry to determinate properties and dynamics of systems in presence of time-depending potentials, like electric or magnetic fields. The traditional density-functional formalism is a powerful tool in predicting ground-state properties of many-electron systems. The description of excited-state properties within DFT, however, is notoriously difficult. Several extensions of ground-state DFT have been devised to tackle excited states (Petersilka *et al.*, 1996). TD-DFT includes those extensions and is now well-known as a rigorous formalism for the treatment of excitation energies within the DFT framework (Jamorski Jödicke and Lüthi,

2003). As an extension to DFT, TD-DFT provides information about excitation energies, frequency-dependent response properties and photo-absorption spectra.

For this research, TD-DFT calculations were performed in order to predict the UV-VIS spectra. The energy required to reach the first excited state from ground state is calculated as a vertical excitation energy, which means the molecule geometry stays intact. However, that same structure does not necessarily match the excited state minimum, *i.e.* geometry optimization is required to have, if exists, such minimum on the excited PES (Figure 5).
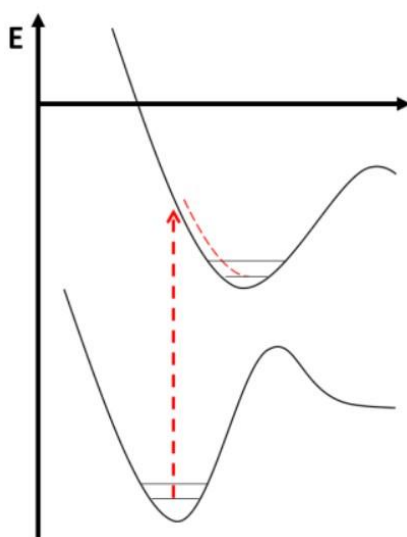
Figure 5. Vertical excitation does not match excited state minimum.

3.9   Solvation calculations

Reactions that were examined in this work, just like most of reactions in general, take place in solution. Geometry optimization, together with frequency calculation, provides with energy and molecular structure in vacuum, so to describe a real reaction it is necessary to use solvation models to take solvent-molecule interactions into account as well. Solvation can alter the properties of a molecule, *e.g.* its charge distribution, geometry, vibrational frequencies, electronic transition energies, NMR constants, chemical reactivity, so it is mandatory to pick the best suitable solvation model. Molecules of solvent can also be reactants or catalysts. In this work, the most important information gathered from these calculations are solvation free energies.

3.9.1 Implicit and explicit solvation

There are two possibilities to determinate solvation effects: implicit and explicit solvation. Implicit solvation implies the polarizable continuum model (PCM). The solvation process in these models is viewed as a series of the following processes: formation of a solvation cavity in a polarizable continuum, entry of the observed molecule into the formed cavity, and relaxation of the continuum around the molecule (Bachrach, 2014). The cavity is defined by overlapping Van der Waals spheres, having an isodensity surface which is solvent-accessible. Commonly used PCM model, also used in this work, is solvation model based on density (SMD). It is a universal model, which means it is applicable to any charged or uncharged solute in any solvent or liquid medium for which a few key descriptors are known (*e.g.* dielectric constant). The SMD model is based on the quantum mechanical charge density of a solute molecule interacting with a continuum description of the solvent. The SMD model achieves mean unsigned errors of 2.4 - 4.0 kJ/mol in solvation free energies of tested neutrals and mean unsigned errors of 25 kJ/mol on average for ions, whereas other default solvation methods have unsigned errors of 4 - 25 kJ/mol for these neutrals and 30 - 42 kJ/mol for ions (Marenich *et al.*, 2009).

Explicit solvation implies direct, specific solvent interactions with a solute, in contrast to continuum models. Unlike the implicit approach where solvent is not in contact with the system, this method simulates solvation shells (the first solation shell mostly) which are in immediate contact with the molecule. For each chemical structure it is required to determinate the optimal number of solvent molecules in the solvation shell, the resulting structure is then considered as a unique chemical species (Tandarić, 2016).

3.9.2 uESE and xESE solvation method

To make sure unsigned errors SMD method carries (especially for charged species) did not significantly impact the results, uESE (universal easy solvation energy evaluation) solvation method (Vyboishchikov, 2021; Vyboishchikov and Voityuk, 2020; Voityuk and Vyboishchikov, 2019) was used. The model takes into account non-electrostatic contributions, which depend on atomic surfaces, induced surface charge densities, and the molecular volume. uESE exhibits an excellent performance, which is superior to major solvation methods. The mean absolute error of predicted solvation energies is found below 4 kcal/mol for neutral solutes and below 12 kcal/mol for ions. The calculated data are almost independent of the quantum-

chemical method or/and basis sets employed (Vyboishchikov and Voityuk, 2021). uESE method requires as input Cartesian coordinates and CM5 atomic charges only, which are easily available from any DFT calculation, and yields the solvation energy in a matter of seconds for a medium-size molecule or ion. The version of the method for aqueous solution program is called xESE, for which calculation time is even shorter.

3.10 Calculation of acid dissociation equilibria

Acid dissociation constants, also known as pK_a values, are essential for understanding many fundamental reactions in chemistry and biochemistry. These values reveal the deprotonation state of a molecule in a particular solvent. For a weak acid dissociation in water:

$$HA_{(aq)} \leftrightharpoons A_{(aq)}^- + H_{(aq)}^+ \quad (1a)$$

or

$$HA_{(aq)} + H_2O_{(l)} \leftrightharpoons A_{(aq)}^- + H_3O_{(aq)}^+ \quad (1b)$$
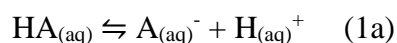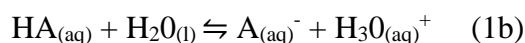
pK_a is defined for equation (1a) as:

$$pK_a = -\log K_a \quad (2)$$

$$K_a = \frac{[A_{(aq)}^-]_{eq}\,[H_{(aq)}^+]_{eq}}{[HA_{(aq)}]_{eq}} \quad (3)$$

The equilibrium constant K_a, can also be calculated using Gibbs free energies at a certain pressure and temperature:

$$K_a = e^{-\frac{\Delta G^*_{total}}{RT}} = e^{-\frac{G^*_{A-(aq)}+G^*_{H+(aq)}-G^*_{HA(aq)}}{RT}} \quad (4)$$

where R stands for the universal gas constant, T for the temperature in Kelvin scale, and the asterisk (*) next to Gibbs free energies (G) represents solution standard state. From equation 2 and 4 it follows:

$$pK_a = -\log K_a = \frac{\Delta G^*_{total}}{\log(10)RT} = \frac{G^*_{A^-(aq)} + G^*_{H^+(aq)} - G^*_{HA(aq)}}{2.303RT} \quad (5)$$

Even though pK$_a$ values can be easily experimentally measured for many chemical systems. For molecules that have not been synthesized, those for which experimental pK$_a$ determinations are difficult, and for larger molecules where the local environment changes the usual pK$_a$ values, there is a great interest in using theoretical methods to calculate those pK$_a$ values. What makes it complicated is the fact that small discrepancies between real and calculated free energy can result in significant pK$_a$ errors. 6 kJ/mol in the change of free energy for deprotonation in solvent results in difference of one pK$_a$ unit (Alongi and Shields, 2010). In this work, pK$_a$ was calculated using six different methods to compare them and to get the most accurate results. In all cases temperature was fixed at 25°C, *i.e.* 298.15K, 1 atm for pressure and 1 mol·dm^{-3} as standard states for the gas phase and aqueous solution, respectively.

3.10.1 <u>Method 1</u>. Thermodynamic cycle involving gas phase and aqueous solution calculations using chemical equilibrium 1a.

The first method is also the one most commonly used. pK$_a$ values are calculated following the thermodynamic cycle shown in Figure 6, which corresponds to the chemical equilibrium (1a).

$$AH(g) \rightleftharpoons A^-(g) + H^+(g)$$
$$\updownarrow \qquad\qquad \updownarrow \qquad\qquad \updownarrow$$
$$AH(aq) \rightleftharpoons A^-(aq) + H^+(aq)$$
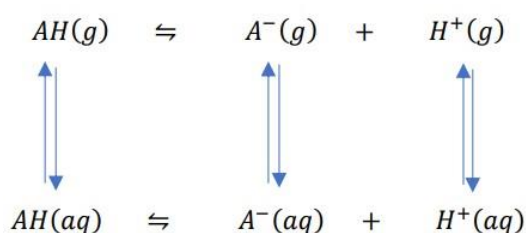
Figure 6. Thermodynamic cycle for calculating pK$_a$ using gas and solution phase species.

In this case, pK$_a$ values are calculated using both gas and solution phase calculations. For the gas phase part, the change in gas phase Gibbs free energy (ΔG_{gas}) is obtained using calculated Gibbs free energies of each species in the chemical equilibria:

$$\Delta G_{gas} = G^°_{A^-(g)} + G^°_{H^+(g)} - G^°_{AH(g)} \quad (6)$$

The next step is to calculate the change in solvation free energy (ΔG_{solv}):

$$\triangle G_{solv} = \triangle G_{solvA-} + \triangle G_{solvH+} - \triangle G_{solvAH}$$

where the solvation free energies gathered from the difference between the electronic energies of species in gas phase and solution phase:

$$\triangle G_{solvAH} \approx E_{el,\ AH(aq)} - E_{el,AH(g)}$$

$$\triangle G_{solvA-} \approx E_{el,\ A^-(aq)} - E_{el,A^-(g)}$$

Since H^+ has no electrons, it is impossible to determinate $G^{\circ}_{H+(g)}$ and $\triangle G_{solvH+}$ using quantum chemical calculations. For this reason, for proton description it is necessary to use experimental data. For the absolute free energy of proton in gas phase the value of -26.28 kJ/mol was used (obtained with the Sackur-Tetrode equation), while for the Gibbs energy of proton in water solution the value -265.9 kcal/mol was taken into account. This latter value is proven to be the most accurate one according to literature. The conversion from gas-phase standard state (1 atm) to solution standard state (1 mol·dm^{-3}) is done by adding 1.89 kcal/mol to the calculation. Considering all from above, $\triangle G_{solvH+}$ was calculated as:

$$\triangle G_{solvH+} = \text{-26.28}\ \frac{kJ}{mol} + (-265.9\ \frac{kcal}{mol} + 1.89\frac{kcal}{mol}) \cdot 4.184\ \frac{kJ}{kcal} = 1130.9\ \frac{kJ}{mol}$$
$$\triangle G_{solvH+} = 1130.9\ \frac{kJ}{mol}$$

Therefore $\triangle G_{total}$ is:

$$\triangle G_{total} = \triangle G_{gas} + \triangle G_{solv}$$

and pK$_a$ is then calculated using equation 5 (Psciuk *et al.*, 2012).

3.10.2 <u>Method 2.</u> Direct method using calculated Gibbs free energies in solution for the chemical equilibrium 1a.

An alternative approach to method 1 is to estimate pK$_a$ using Gibbs free energies of the optimized structures in solution only together with the proton solvation energy (the same as in

method 1), again chemical equilibrium (1a) is being considered. To get the acidity constant, the values are then inserted into equation 5.

3.10.3 <u>Method 3.</u> Isodesmic method

Acidity constants in this method are estimated with respect to the pKa of a reference acid of known experimental pK_a:

$$HTh_{(aq)} + A^-_{(aq)} \leftrightarrows AH_{(aq)} + Th^-_{(aq)}$$
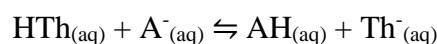
The significant advantage of this approach is error cancellation achieved by using the same functionals and basis set for the acid of interest and reference acid. In this research thiazolidine (Th) was taken as reference. $\triangle G_{total}$ is obtained as:

$$\triangle G_{total} = G_{AH(ag)} + G_{Th^-(aq)} - G_{HTh(aq)} - G_{A^-(aq)}$$

In the end, with $\triangle pK_a$ estimated by equation 5, pK_a is calculated as:

$$pK_a = pK_a - \triangle pK_a \text{ (Casasnovas } et\ al., 2014)$$

3.10.4 <u>Method 4.</u> Direct method using calculated Gibbs free energies in solution for the chemical equilibrium 1b.

Following method 2, this one uses Gibbs free energies of solvated species to calculate $\triangle G_{total}$, but now for chemical equilibrium (1b):

$$\triangle G_{total} = G_{A^-(aq)} + G_{H3O+(aq)} - G_{AH^-(aq)} - G_{H2O(l)}$$

pK_a is, again, calculated with equation 5, with the logarithm of water molarity (55.56) subtracted from the value as this constant is not included in the equation.

3.10.5   Method 5. Thermodynamic cycle involving gas phase and aqueous solution calculations using chemical equilibrium (1b).

This method is analogous to method 1, with the logarithm of water molarity subtracted as in previous method. It follows the thermodynamic cycle shown in Figure 7.

$$AH(g) \quad + \quad H_2O\,(v) \quad \leftrightharpoons \quad A^-(g) \quad + \quad H_3O^+(g)$$

$$AH(aq) \quad + \quad H_2O(l) \quad \leftrightharpoons \quad A^-(aq) \quad + \quad H_3O^+(aq)$$
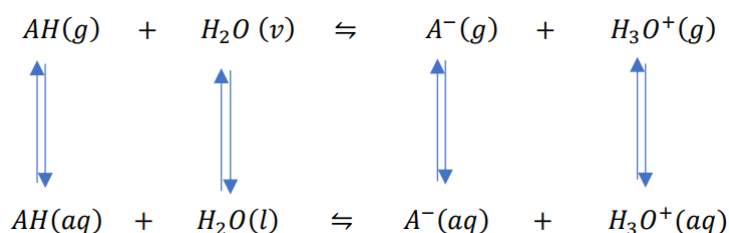
Figure 7. Thermodynamic cycle for calculating pK_a using gas and solution phase species, with explicit water molecules added.

3.10.6   Method 6. Thermodynamic cycle involving gas phase and aqueous solution calculations, using empirical solvation free - energy values for H₂O and H₃O⁺, in chemical equilibrium (1b).

Calculation of pK_a values is similar to method 5, except solvation free energy for H_2O and H_3O^+. Here -26.44 and -461.08 kJ/mol were used for water and hydronium ion, respectively (Casasnovas *et al.*, 2014).

3.11   Chemical equilibrium constants

Chemical equilibrium constants (K_{eq}) for all the reactions observed were calculated using free Gibbs energies of reactants (G_r) and products (G_p) in water solution, at the temperature of 25°C. *i.e.* 298.15 K, following the equation:

$$K_{eq} = e^{-\frac{G_p - G_r}{R \cdot T}} \qquad (6)$$

3.12   Redox potentials

The absolute reduction potential $E^\circ_{red(aq)}$ in aqueous solution can be described by following chemical equilibrium:

$$R^{+\cdot}_{(g)} + e^- \leftrightharpoons R_{(aq)} \qquad (7)$$
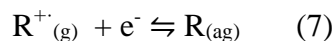
and can be calculated using following equation:

$$E^\circ_{red(aq)} = \frac{-\Delta G^*_{red(aq)}}{nF} \qquad (8)$$

where $\Delta G^*_{red(aq)}$ is the solution phase standard state free energy change, n is the number of electrons exchanged in reaction (in this work always one) and F is the Faraday's constant. For comparison with experimental results, the absolute potential of the standard hydrogen electrode in an aqueous solution ($E^\circ_{(SHE)} = 4.281$ V) has been taken as a reference (Psciuk et $al.$, 2012). As before, temperature was fixed at 25°C. $i.e.$ 298.15 K, 1 atm for pressure and 1 mol·dm^{-3} as standard states for the gas phase and aqueous solution, respectively.

$$R^{+\cdot}_{(g)} + e^- \xrightarrow{\Delta G^*_{red(g)}} R_{(g)}$$

$$R^{+\cdot}_{(aq)} + e^- \xrightarrow{\Delta G^*_{red(aq)}} R_{(aq)}$$
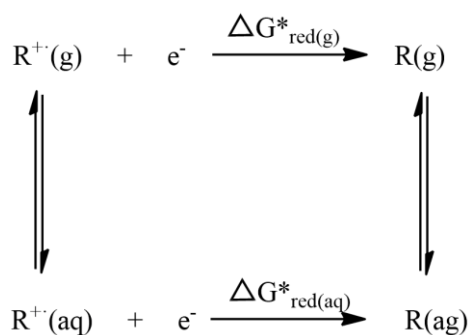
Figure 8. Thermodynamic cycle for calculation of absolute reduction potential in aqueous solution.

Using the thermodynamic cycle in Figure 8, $\Delta G^*_{red(aq)}$ is estimated as:

$$\Delta G^*_{red(aq)} = G^*_{R(aq)} - G^*_{B+(aq)} - G^*_{e-(g)} \qquad (9)$$

where $G^*_{(aq)}$ for both neutral and charged species is calculated as:

$$G*_{(aq)} = (G°_{(g)} + \triangle G^{1atm \rightarrow 1M}) + \triangle G*_{solv} \quad (10)$$

where $\triangle G°^{(g)}$ is the standard state free energy in the gas phase and $\triangle G*_{solv}$ is the standard state free energy of solvation. $\triangle G^{1atm \rightarrow 1M}$ is the free energy difference accounting for the standard state change from the gas phase to solution. After putting equations 9 and 10 together, $\triangle G*_{red(aq)}$ is calculated as:

$$\triangle G*_{red(aq)} = G°_{R(g)} + \triangle G*_{solv(R)} - (G°_{R+(g)} + \triangle G*_{solv(R+)}) \quad (11)$$

The obtained $\triangle G*_{red(aq)}$ value is then used in equation 8 to calculate absolute reduction potential.

3.13 DFT Global reactivity descriptors

DFT based methods can be also used to calculate chemical properties of molecular structures. Using frontier molecular orbitals (FMOs) some parameters have been calculated as follows (Geerlings *et al.*, 2003):

Parameter	Parameter
HOMO-LUMO energy gap	Electronegativity: $\chi = (I + A)/2$
Global chemical hardness: $\eta = (I - A)/2$	Electronic chemical potential: $\mu = - (I + A)/2$
Global chemical softness: $S = 1/2\eta$	Electrophilicity index: $\omega = \mu^2/2\eta$

where, according to Kopmans' theory, ionization potential (I) = $- E_{HOMO}$ and electroaffinity (A) = $- E_{LUMO}$ (Koopmans, 1933).

3.14 Computational programs

Electronic structure calculations were performed in the supercomputer Finis Terrae II, located at the "Centro de Supercomputación de Galicia" (CESGA) (www.cesga.es).
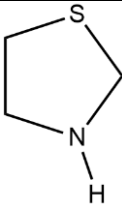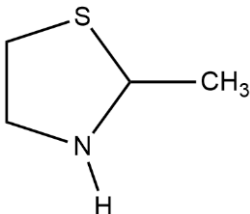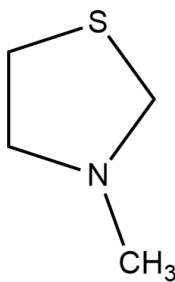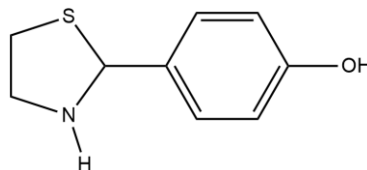
The programs/applications used in this project were the following:

− Supercomputer connection: FortiClient

− Files transfer: SSH Secure Shell Client

− Electronic structure calculations: Gaussian16 (Gaussian, Inc., Wallingford CT, 2016)

− Molecular visualization: GaussView (version 6.0)

− Chemical drawing: ChemDraw Ultra (version 12.0)

− Solvation calculations: xESE program

## 4.	RESULTS AND DISCUSSION

The following molecules have been studied (Table 1):

Table 1. Molecules studied in this work

Chemical structure	Name	IUPAC name	CAS* number	EC** number
	Thiazolidine	1,3-thiazolidine	504-78-9	208-002-5
	2-methyl-thiazolidine	2-methyl-1,3-thiazolidine	24050-16-6	607-310-0
	N-methyl-thiazolidine	3-methyl-1,3-thiazolidine	52288-89-8	-
	2-(4'-hydroxy)-phenyl-thiazolidine	4-(1,3-thiazolidin-2-yl)phenol	31404-07-6	-

*Chemical Abstracts Service; **European Community

The acidity and chemical equilibrium constants studied in this work are shown in Figures 9 and 10. Species are numbered from 1 to 6, and are followed by pK_as and K_{eq}s assignations accordingly. Thiazolidine, 2-methyl-thiazolidine and 2-(4'-hydroxy)-phenyl-thiazolidine have

the same reaction schemes, while N-methyl-thiazolidine has it slightly different due to the presence of a methyl group on the nitrogen atom.


R=H, thiazolidine
R=CH₃, 2-methyl-thiazolidine
R= ⟨◯⟩—OH , 2-(4'-hydroxy)-phenylthiazolidine
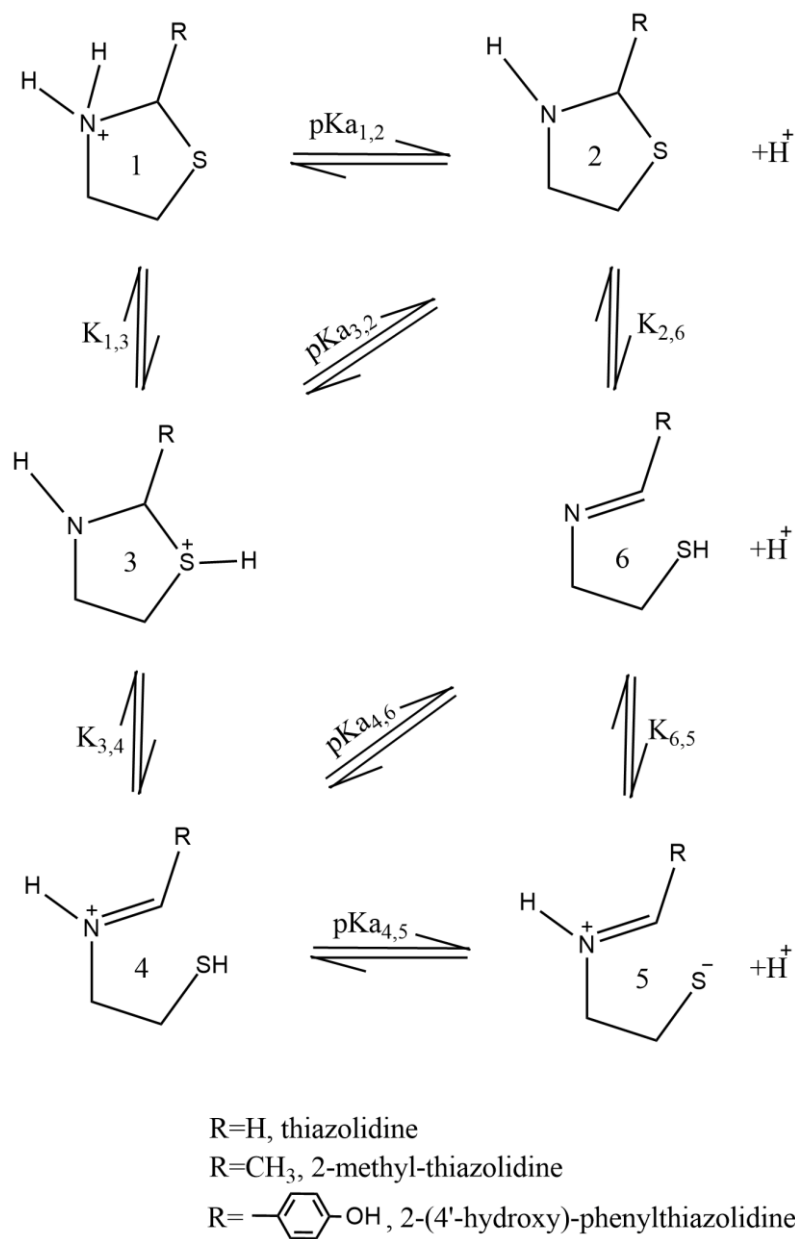
Figure 9. Reaction scheme with studied pK_a and K_{eq} for thiazolidine, 2-methyl-thiazolidine and 2-(4'-hydroxy)-phenyl-thiazolidine.
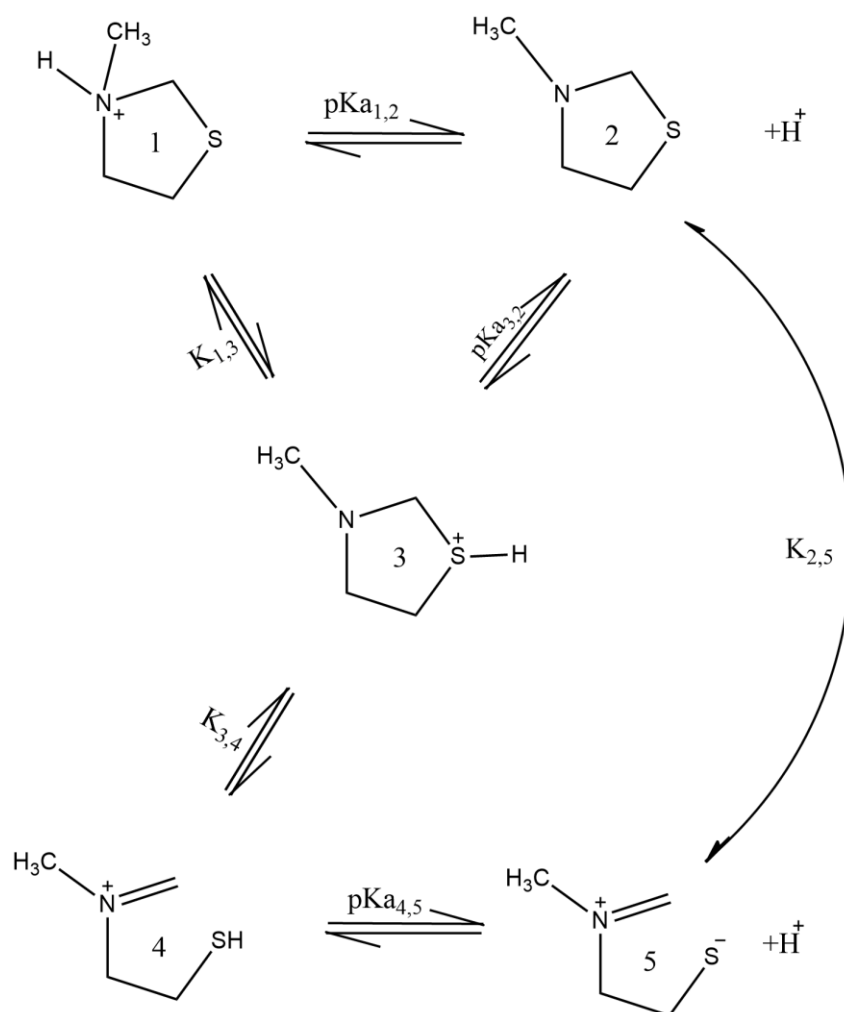
Figure 10. Reaction scheme with studied pK_a and K_{eq} for N-methyl-thiazolidine.

4.1 Acidity constants

Acidity constants were calculated using the methods described in the materials and methods chapter (3.10.). To determine which functional and basis set best describe the studied molecules, $pK_{a(1,2)}$ for thiazolidine was firstly calculated using three different computational methods: b3lyp with 6-31G(d,p), b3lyp with 6-311++G(d,p) and CBS-QB3 composite method, all with SMD solvation model. The reason why only thiazolidine was used among all other molecules is because it is the only one for which the experimental pK_a value is available in the literature (Ratner and Clarke, 1937). The outcome is shown in Table 2, where the acidity constant values are calculated using Method 1, the most commonly used method. Since b3lyp/6-31G(d,p) gave the best result, *i.e.* the closest value to the experimental one, it was used in further calculations.

Table 2. pK$_a$ values calculated with Method 1 for thiazolidine, using b3lyp/6-31G(d,p), b3ylp/6-311++G(d,p) and CBS-QB3, all with SMD solvation model.

	b3lyp/6-31G(d,p)	b3ylp/6-311++G(d,p)	CBS-QB3	Experimental value
pK$_{a(1,2)}$	6.73	3.62	5.08	6.31*

*Ratner and Clarke, 1937

Obtained results for all studied molecules are presented in Table 3. The table includes pK$_a$ values calculated by previously described methods. The experimental value of 6.31 for thiazolidine pK$_{a(1,2)}$ suggests that the best method for thiazolidine and its derivatives is method 5, where SMD solvation calculation is used. xESE calculations were considered in this method also (as it is the most accurate one), but the result did not improve. The purpose of acidity constants calculation is to determine the corresponding speciation. For example, by knowing these information, tuning the pH value of aqueous solution for these molecules, ring-opening or ring-closing reactions can be initiated. Table 3 shows that N-methyl-thiazolidine is the weakest acid, as expected, because of the direct inductive effect provided by methyl group on nitrogen atom making it harder to give the proton away. Again due to the inductive effect of methyl group, 2-methyl-thiazolidine is the second weakest acid, while 2-(4'-hydroxy)-phenyl-thiazolidine is the strongest due to the presence of the aromatic ring. As it follows from the Table 3, pK$_a$ values for all four molecules show the same trend (where pK$_{a(4,6)}$ is determined for first three molecules only):

$$pK_{a(4,5)} > pK_{a(4,6)} > pK_{a(1,2)} > pK_{a(3,2)}$$

pK$_{a(4,5)}$ and pK$_{a(4,6)}$ values, the ones associated with opened-ring molecules, show that with the increase of pH the dissociation of the NH group progresses faster than the dissociation of the SH group. In two other cases, where the behaviour of closed-ring species is described by the acidity constants, SH group is the stronger acid.

All acidity constants were calculated using the energies of optimized molecules (the most stable structure), which means no other conformations contribute to pK$_a$ significantly. Those differences in energies cause insignificant discrepancies in the value when compared to ones derived from solvation energies.

Table 3. pK$_a$ values obtained for thiazolidine, 2-methyl-thiazolidine, 2-(4'-hydroxy)-phenyl-thiazolidine and N-methyl-thiazolidine using the methods described in Materials and methods (3.10.) (b3lyp/6-31G(d,p) level).

| | AH → A$^-$ + H$^+$ | | AH + R$^-$ → A$^-$ + RH | | AH + H2O → A$^-$ + H$_3$O$^+$ | | |
| | Method 1 | Method 2 | Method 3 | Method 4 | Method 5 | | Method 6 |
					SMD	xESE	
Thiazolidine							
pK$_{a(1,2)}$	6.73	6.61	4.76	19.9	6.35	16.91	18.4
pK$_{a(3,2)}$	-2.18	-2.19	-4.05	11.09	-2.56	-0.63	9.49
pK$_{a(4,6)}$	9.24	9.72	7.86	23.00	8.86	11.40	20.91
pK$_{a(4,5)}$	19.17	20.06	18.20	33.35	18.79	29.59	30.84
2-methyl-thiazolidine							
pK$_{a(1,2)}$	6.96	6.82	4.07	20.11	6.58	5.07	18.63
pK$_{a(3,2)}$	3.93	3.71	1.85	17.00	3.55	6.54	15.60
pK$_{a(4,6)}$	12.81	13.23	11.37	26.51	12.42	11.47	24.48
pK$_{a(4,5)}$	19.56	20.50	18.65	33.79	19.18	40.80	31.23
2-(4'-hydroxy)-phenyl-thiazolidine							
pK$_{a(1,2)}$	6.45	6.13	4.27	19.42	6.06	5.07	18.12
pK$_{a(3,2)}$	6.15	7.79	5.93	21.07	5.77	6.54	17.82
pK$_{a(4,6)}$	14.28	14.52	12.67	27.81	13.90	11.47	25.95
pK$_{a(4,5)}$	35.39	35.94	34.08	49.22	35.00	40.80	47.06
N-methyl-thiazolidine							
pK$_{a(1,2)}$	8.03	7.70	5.83	20.98	7.65	7.58	19.70
pK$_{a(3,2)}$	0.73	0.49	-1.73	13.77	0.35	-0.89	12.40
pK$_{a(4,5)}$	19.23	19.87	18.02	33.16	18.85	27.18	30.90

4.2 Chemical equilibrium constants

To find out in which amount each of the six (or five in case of N-methyl-thiazolidine) studied species exists and to determine the direction of chemical reactions presented in Figures 9 and 10, chemical equilibrium constants (K$_{eq}$) were calculated. All K$_{eq}$ values were obtained from Gibbs free energies calculated by b3lyp/6-31G(d,p) method and basis set, as it was already proven to be the most accurate one. For the same reason, SMD solvation model was used. In

the reaction scheme, there are two types of reactions: charge/proton transfer and ring opening-closure.

From Table 4 the following conclusions are drawn:

1. For reaction 1 to 3, closed-ring charge/proton transfer, reverse reaction is preferable in all molecules but 2-(4'-hydroxy)-phenyl-thiazolidine. This is understandable due to the higher electronegativity of the nitrogen atom compared to that of sulphur. On the other hand, nitrogen's free electron pair could contribute in conjugated system in 2-(4'-hydroxy)-phenyl-thiazolidine, which makes species 3 more stable than species 1.

2. For reaction 6 to 5, opened-ring charge/proton transfer, reverse reaction is preferable for all molecules. This was, again, expected since molecule 5 bears two separated charges.

3. For reaction 3 to 4, the ring opening is preferable to the ring closure in all molecules.

4. For reaction 2 to 6, the ring closure is preferable to the ring opening in all molecules. The same result is obtained for reaction 2 to 5 for N-methyl-thiazolidine.

Table 4. Chemical equilibrium constants (K_{eq}) of chemical reactions shown in Figures 9 and 10 calculated at b3lyp/6-31G(d,p)/SMD level.

K_{eq}	Thiazolidine	2-methyl-thiazolidine	2-(4'-hydroxy)-phenyl-thiazolidine	N-methyl-thiazolidine
$K_{eq(1,3)}$	$1.56 \cdot 10^{-9}$	$7.71 \cdot 10^{-4}$	45.43	$6.16 \cdot 10^{-8}$
$K_{eq(6,5)}$	$4.54 \cdot 10^{-9}$	$5.31 \cdot 10^{-8}$	$3.85 \cdot 10^{-22}$	-
$K_{eq(2,6)}$	$1.92 \cdot 10^{-10}$	$6.04 \cdot 10^{-7}$	$4.00 \cdot 10^{-4}$	-
$K_{eq(3,4)}$	$1.55 \cdot 10^{2}$	$1.99 \cdot 10^{3}$	$21.56 \cdot 10^{2}$	38.11
$K_{eq(2,5)*}$	-	-	-	$1.57 \cdot 10^{-18}$

*N-methyl-thiazolidine only

4.2.1   Ring-opening reaction

The thiazolidine ring-opening has been examined on 2-(4'-hydroxy)-phenyl-thiazolidine for reaction 2 to 6. From $K_{eq(2,6)}$, and now also from Figure 11, the closed-ring species is 18.5 kJ/mol more stable than the opened-ring one. Once species 2 gets enough energy to cross the 42.4 kJ/mol barrier, C-S bond breaks. Transition state shows electron delocalization between N, C and phenyl ring, all atoms being in planar position.
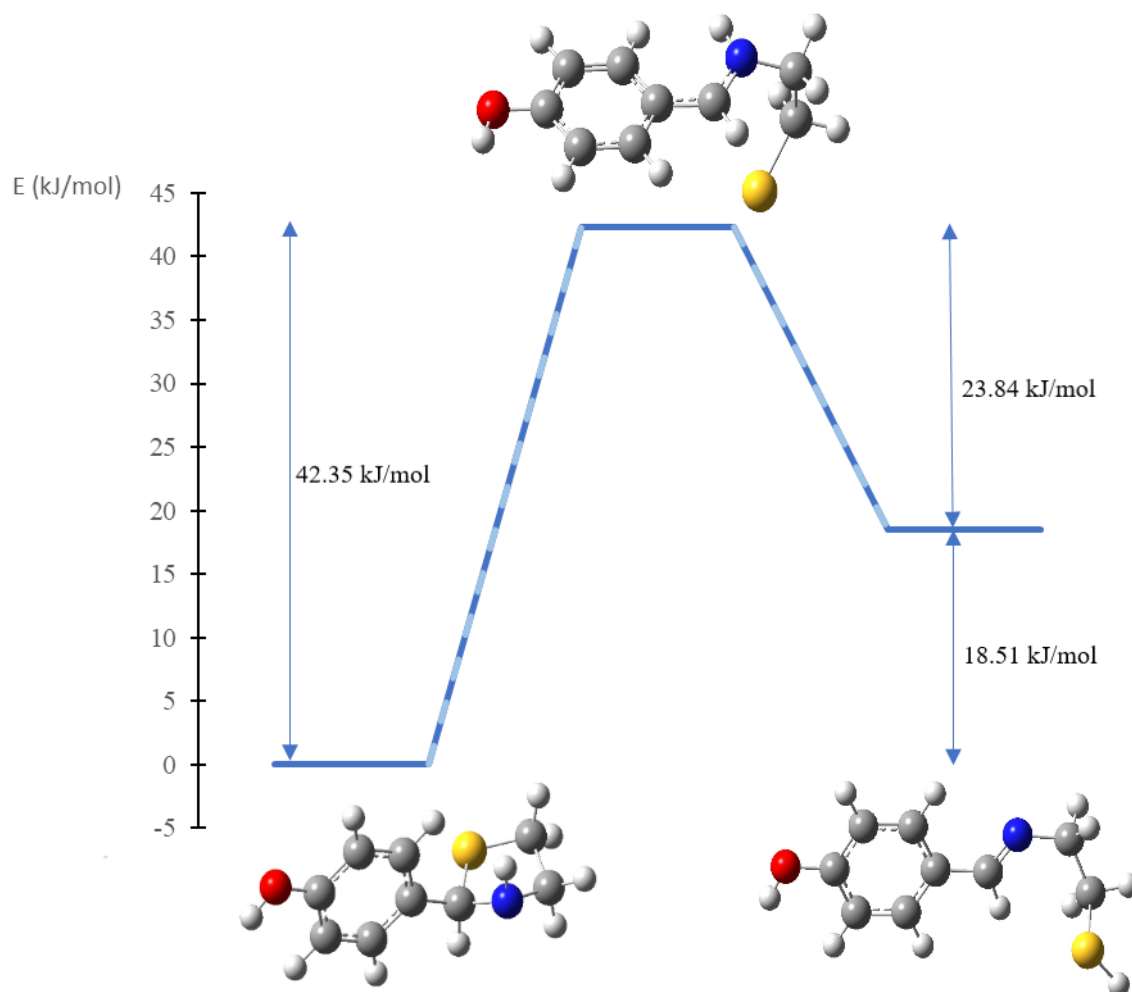
Figure 11. Graphical representation of relative energy relations of minimum and transition state for ring opening of 2-(4'-hydroxy)-phenyl-thiazolidine (b3lyp/6-31G(d,p)/SMD level).

Finally, when the reaction ends, the ring is fully opened, a double C=N bond is formed, sulphur atom drifts away and phenyl ring rotates to be planar with the so formed C=N bond.

4.2.2 DFT Global reactivity descriptors

The frontier molecular orbital (FMO) energies of compounds were calculated by b3lyp/6-31G(d,p) level. It is well known that HOMO (*i.e.* highest occupied molecular orbital) energy relates to the electron giving ability, while LUMO (*i.e.* lowest unoccupied molecular orbital) energy relates to the electron withdrawing ability.

Table 5. HOMO-LUMO energy gap, chemical hardness (η), softness (S), chemical potential (μ), electronegativity (χ) and electrophilicity index (ω) calculated at b3lyp/6-31G(d,p)/SMD level. All values are expressed in eV. Numbers from 1 to 6 represent the species shown in Figures 9 and 10.

	HOMO-LUMO energy gap	η	S	μ	X	ω
Thiazolidine						
1	0.206	0.103	9.709	-0.139	0.139	0.094
2	0.246	0.123	8.135	-0.090	0.090	0.033
3	0.190	0.095	10.542	-0.170	0.170	0.153
4	0.178	0.089	11.261	-0.169	0.169	0.162
5	0.082	0.041	24.254	-0.114	0.114	0.158
6	0.234	0.117	8.533	-0.118	0.118	0.059
2-methyl-thiazolidine						
1	0.250	0.125	8.007	-0.124	0.124	0.061
2	0.243	0.121	8.237	-0.091	0.091	0.034
3	0.198	0.099	10.122	-0.161	0.161	0.131
4	0.184	0.092	10.875	-0.157	0.157	0.134
5	0.096	0.048	20.745	-0.105	0.105	0.115
6	0.244	0.122	8.211	-0.113	0.113	0.052
2-(4'-hydroxy)-phenyl-thiazolidine						
1	0.212	0.106	9.415	-0.126	0.126	0.074
2	0.204	0.102	9.804	-0.108	0.108	0.057
3	0.156	0.078	12.818	-0.162	0.162	0.167
4	0.156	0.078	12.825	-0.164	0.164	0.173
5	0.078	0.039	25.743	-0.117	0.117	0.175
6	0.182	0.091	10.972	-0.126	0.126	0.087
N-methyl-thiazolidine						
1	0.245	0.122	8.171	-0.119	0.119	0.058
2	0.245	0.122	8.174	-0.091	0.091	0.034
3	0.187	0.094	10.691	-0.165	0.165	0.146
4	0.177	0.088	11.300	-0.164	0.164	0.151
5	0.088	0.044	22.774	-0.111	0.111	0.141

Energy gap between HOMO and LUMO relates to the molecular chemical stability and it plays a critical role in determining molecular electrical transport properties (Avci *et al.*, 2016). As stated in the previous chapter, using HOMO and LUMO energies ionization potential (I) and electron affinity (A) can be estimated as $I = -E_{HOMO}$, $A = -E_{LUMO}$ (Koopmans, 1933).

Chemical hardness (η), chemical softness (S), chemical potential (μ), electronegativity (χ) and electrophilicity index (ω) were calculated for all molecules and are presented in Table 5.

As for pK_a and K_{eq} values, the same ratio of energy gap values for species 1 to 6 is present between the individual molecules studied.

For species 1, 2 and 6, the HOMO-LUMO values are rather similar for each molecule and represent the species with the largest HOMO-LUMO energy gap. They are followed by species 3 and 4, which also have similar values. Finally, species 5 shows the lowest value for all molecules studied.

Considering the obtained numbers, charge transfer occurs in all compounds. Species 5 is more reactive than the others, while species 1,2 and 6 are the least reactive. It can also be observed that 2-(4'-hydroxy)-phenyl-thiazolidine has the lower values for all species, which means it should be the most reactive molecule among the studied.

4.3   TD-DFT calculations

To predict which wavelength and light intensity are required to get the molecules into the first excited electronic state, TD-DFT calculations were performed. Once the molecule absorbs the HOMO-LUMO amount of energy, ring-opening could occur. All calculations were carried at b3lyp/6-31G(d,p) level, using SMD to simulate water solvation.

The results in Table 6 include three wavelengths with the highest oscillator strength for each of the species studied. Results follow HOMO-LUMO energy gap values from Table 5, as expected. Species 5 has the highest wavelength, *i.e.* it requires the lowest amount of energy to get to the excited state, which corresponds to the lowest energy gap. On the other hand, lower wavelengths are found for species 1, 2 and 6.

Table 6. Wavelength (λ) with corresponding oscillator strength (f) calculated at b3lyp/6-31G(d,p)/SMD level.

Species	Thiazolidine		2-methyl-thiazolidine		2-(4'-hydroxy)-phenyl-thiazolidine		N-methyl-thiazolidine	
	λ\ nm	f	λ\ nm	f	λ\ nm	f	λ\ nm	f
1	239.61	0.0143	240.89	0.0110	239.31	0.1217	248.77	0.0041
	222.70	0.0255	221.11	0.0290	208.18	0.1059	222.67	0.013
	196.43	0.0361	197.12	0.0310	206.43	0.1069	193.95	0.0164
2	215.01	0.0173	223.3	0.0139	226.22	0.0742	220.22	0.0296
	203.99	0.0379	207.78	0.0243	222.12	0.0571	216.25	0.0219
	198.78	0.0103	201.96	0.0141	219.07	0.0498	201.28	0.0097
3	252.27	0.0047	254.71	0.0034	250.25	0.0463	266.63	0.0023
	247.55	0.0100	242.21	0.0057	239.31	0.1811	252.83	0.0283
	193.01	0.0276	193.24	0.0237	204.69	0.1134	199.73	0.0363
4	494.23	0.0201	360.54	0.0763	400.81	0.1188	365.58	0.0839
	250.98	0.0032	217.73	0.0132	302.37	0.4495	229.41	0.0009
	234.69	0.0011	207.36	0.0044	294.71	0.1047	217.29	0.0098
5	630.27	0.2076	674.51	0.2011	448.04	0.0114	691.15	0.1754
	278.32	0.0281	277.79	0.0314	420.82	0.0274	402.26	0.0146
	252.6	0.0364	273.93	0.0517	329.22	0.1295	280.33	0.0297
6	257.92	0.0015	222.71	0.0106	267.80	0.2584	-	-
	243.06	0.0042	212.82	0.0115	255.51	0.2244	-	-
	235.63	0.0051	202.89	0.0059	215.45	0.0906	-	-

4.4 Redox potentials

One-electron reduction potential calculations ($R^+ + e^- \rightarrow R$) were carried out for all molecules and are collected in Table 7. As stated in Chapter 3, absolute one-electron reduction potentials were calculated, but for comparison purposes, they have been reported as values relative to SHE. Since obtained values seem independent on the basis set used, unlike the results in previously listed tables, here presented are results for b3lyp with both 6-31G(d,p) and 6-311++G(d,p).

Table 7. E° values (V), relative to SHE, obtained for thiazolidine, 2-methyl-thiazolidine, 2-(4'-hydroxy)-phenyl-thiazolidine and N-methyl-thiazolidine calculated at b3lyp/6-31G(d,p) and b3lyp/6-311++G(d,p) level, both with SMD solvation.

Numbers from 1 to 6 represent the species in Figures 9 and 10.

b3lyp/	$R^+ + e^- \rightarrow R$					
	1	2	3	4	5	6
Thiazolidine						
6-31G(d,p)	-10.92	-9.95	-11.51	-11.10	-8.46	-10.18
6-311++G(d,p)	-10.98	-10.14	-11.12	-11.14	-8.97	-10.37
2-methyl-thiazolidine						
6-31G(d,p)	-10.87	-9.89	-11.38	-11.12	-8.44	-10.05
6-311++G(d,p)	-10.93	-10.08	-10.93	-11.17	-8.76	-10.25
2-(4'-hydroxy)-phenyl-thiazolidine						
6-31G(d,p)	-10.20	-9.70	-10.45	-10.54	-8.52	-9.82
6-311++G(d,p)	-10.44	-9.95	-10.89	-10.74	-8.83	-10.11
N-methyl-thiazolidine						
6-31G(d,p)	-10.90	-9.53	-11.34	-11.16	-8.50	-
6-311++G(d,p)	-10.95	-9.72	-11.18	-11.21	-8.80	-

Reduction potentials, when compared between different molecules, are similar and follow the same trend for species 1 to 6. For all molecules, species number 3 and 4 have the highest reduction ability, while species number 5 has the lowest.

5.   CONCLUSION

An experimental study on thiazolidine, 2-methyl-thiazolidine, 2-(4'-hydroxy)-phenyl-thiazolidine and N-methyl-thiazolidine revealed that the thiazolidine ring can be opened using UV light. Since the reaction is fast with unstable products, and the process has high potential for various uses, there was a need for an additional understanding of the observed phenomenon. In this study, chemical parameters essential for understanding the deprotonation and thiazolidine ring opening reactions are collected using computational techniques on the mentioned molecules. For each molecule, six different species (numbered one to six) (five in case of N-methyl-thiazolidine) geometries were optimized using three different computational methods: b3lyp/6-31G(d,p), b3lyp/6-311++G(d,p) and CBS-QB3. Acidity constants, using six different methods, equilibrium constants, reduction potentials, a transition state for a thiazolidine ring opening, an IRC, DFT Global reactivity descriptors and excitation energies were calculated.

The results gathered in this work are the following:

1. After comparing the results with experimental ones, b3lyp/6-31G(d,p) was proven to be the most accurate method for all calculations apart from redox one, where both b3lyp/6-31G(d,p) and b3lyp/6-311++G(d,p) showed similar results.

2. Two implicit solvation models were tested, xESE and SMD methods. SMD provided better results and was therefore used.

3. Methods 1, 2, and 5, with SMD solvation, used for pK_a calculations seem the most reliable; method 5 provided the closest value to the known experimental thiazolidine's pK_a.

4. As assumed by observing the molecular structures, pK_a values show the following order of acid strength from weakest to strongest: N-methyl-thiazolidine, 2-methyl-thiazolidine, thiazolidine, 2-(4'-hydroxy)-phenyl-thiazolidine. Furthermore, pK_a values for all molecules follow the same trend: $pK_{a(4,5)} > pK_{a(4,6)} > pK_{a(1,2)} > pK_{a(3,2)}$.

5. Chemical equilibrium constants indicate that for three out of four reactions observed reverse process is preferable. These reactions include charge/proton transfer for both closed and opened ring species (reactions 1-3 and 6-5), and ring opening reaction 2-6 (2-5 for N-methyl-thiazolidine). The only exception is reaction 1-3 for 2-(4'-hydroxy)-phenyl-thiazolidine. On the other hand, reaction 3-4, *i.e.* ring-opening reaction, is going forward for all molecules.

6. IRC calculation gave the insight into the transition state of ring-opening reaction with an activation energy of *ca.* 40 kJ/mol. After the C-S bond in thiazolidine ring breaks, electron delocalization between N, C and phenyl ring occurs, leading to imine formation followed by phenyl ring rotation and sulphur atom drifting away.

7. Calculated global reactivity indexes follow the same pattern for all molecules. Species 5 is the most reactive; followed by species 3 and 4, while 1, 2 and 6 are the less reactive.

8. TD-DFT calculation results confirm what reactivity indexes showed. Species 5 requires the lowest amount of energy to get the excited state. On the other hand, lower wavelengths are found for species 1, 2 and 6. Species 3 and 4 require energy between the two listed to reach the first excited state.

9. Reduction potentials, when compared between different molecules, are similar and follow the same trend for species 1 to 6. For all molecules, species 3 and 4 have the highest reduction ability, while number 5 has the lowest.

6. REFERENCES

Alongi KS, Shields GC. Theoretical Calculations of Acid Dissociation Constants: A Review Article. *Annual Reports in Computational Chemistry,* 2010, 6, 113–138.

Avci D, Tamer Ö, Atalay Y. Solvatochromic effect on UV–vis absorption and fluorescence emission spectra, second- and third-order nonlinear optical properties of dicyanovinyl-substituted thienylpyrroles: DFT and TDDFT study. *Journal of Molecular Liquids*. 2016, 220, 495-503.

Bachrach SM. Computational Organic Chemistry. 2nd ed., New Jersey, John Wiley & Sons, 2014, 29-40.

Becke AD. Density-functional exchange-energy approximation with correct asymptoticbehavior. *Phys Rev A*, 1988, 38, 3098-3100.

Bengtsson-Palme J, Milaković M, Švecová H, Ganjto M, Jonsson V, Grabić R, Udiković-Kolić N. Industrial wastewater treatment plant enriches antibiotic resistance genes and alters the structure of microbial communities. *Water research,* 2019, 162, 437-445.

Casasnovas R, Ortega-Castro J, Frau J, Donoso J, Munoz F. Theoretical pK(a) Calculations With Continuum Model Solvents, Alternative Protocols to Thermodynamic Cycles. *Int. J. Quantum Chem*. 2014, 114, 1350-1363.

Centro de Supercomputación de Galicia (CESGA), 1993, https://www.cesga.es/. Last access 31/08/2021.

Davis AM, Layland NJ, Page M, Martin F, O'Ferrall RM. Thiazolidine Ring Opening in Penicillin Derivatives. Part 2. Enamine Formation. *J. Chem. Soc. Perkin Trans. 2*. 1991, 1225-1229.

De Metrio G, Corriero A, Desantis S, Zubani D, Cirillo F, Deflorio M, Bridges CR, Eicker J, de la Serna JM, Megalofonou P, Kime DE. Evidence of a high percentage of intersex in the Mediterranean swordfish (Xiphias gladius L.). *Marine Pollution Bulletin*, 2003, 46(3), 358–361.

Fife TH, Natarajan R, Shen CC, Bembi R. Mechanism of Thiazolidine Hydrolysis. Ring Opening and Hydrolysis of 1,3-Thiazolidine Derivatives of p-(Dimethy1amino)cinnamaldehyde. *J. Am. Chem. SOC*, 1991, 113, 3071-3079.

Filipović K. Diplomski rad: Usporedba DFT metoda za računanje elektrokemijskih parametara ferocenskih derivata. Farmaceutsko-biokemijski fakultet Sveučilišta u Zagrebu, 2018.

Foresman JB, Frisch A. Exploring chemistry with electronic structure methods. 2nd ed., Gaussian, Inc., Pittsburgh, PA, 1996, 3-90.

Fukui K. The path of chemical-reactions - The IRC approach. Acc Chem Res, 1981, 14, 363-368.

Gaussian 16, Revision C.01. Frisch MJ, Trucks GW, Schlegel HB, Scuseria GE, Robb MA, Cheeseman JR, Scalmani G, Barone V, Petersson GA, Nakatsuji H, Li X, Caricato M, Marenich AV, Bloino J, Janesko BG, Gomperts R, Mennucci B, Hratchian HP, Ortiz JV, Izmaylov AF, Sonnenberg JL, Williams-Young D, Ding F, Lipparini F, Egidi F, Goings J, Peng B, Petrone A, Henderson T, Ranasinghe D, Zakrzewski VG, Gao J, Rega N, Zheng G, Liang W, Hada M, Ehara M, Toyota K, Fukuda R, Hasegawa J, Ishida M, Nakajima T, Honda Y, Kitao O, Nakai H, Vreven T, Throssell K, Montgomery JA Jr., Peralta JE, Ogliaro F, Bearpark MJ, Heyd JJ, Brothers EN, Kudin KN, Staroverov VN, Keith TA, Kobayashi R, Normand J, Raghavachari K, Rendell AP, Burant JC, Iyengar SS, Tomasi J, Cossi M, Millam JM, Klene M, Adamo C, Cammi R, Ochterski JW, Martin RL, Morokuma K, Farkas O, Foresman JB, Fox DJ. Gaussian, Inc., Wallingford CT, 2016.

Geerlings, P., De Proft, F., Langenaeker, W. Conceptual Density Functional Theory. *Chemical Reviews*, 2003, 103(5), 1793-1874.

Hok L. Mehanizam reakcije kloriranja 5-fluorouracila i ekotoksikološka analiza kloriranih produkata. Farmaceutsko-biokemijski fakultet Sveučilišta u Zagrebu, 2017.

Jamorski Jödicke C, Lüthi HP. Time-Dependent Density Functional Theory (TDDFT) Study of the Excited Charge-Transfer State Formation of a Series of Aromatic Donor−Acceptor Systems. *Journal of the American Chemical Society*, 2003, 125(1), 252–264.

Koopmans, T. über die Zuordnung von Wellenfunktionen und Eigenwerten zu den Einzelnen Elektronen Eines Atoms. *Physica*, 1933, 1(1-6), 104-113.

Li WC. Occurrence, sources, and fate of pharmaceuticals in aquatic environment and soil. *Environmental Pollution,* 2014, 187*,* 193–201.

Marenich AV, Cramer CJ, Truhlar DG. Universal Solvation Model Based on Solute Electron Density and on a Continuum Model of the Solvent Defined by the Bulk Dielectric Constant and Atomic Surface Tensions. *J. Phys. Chem.*, 2009, 113(18), 6378–6396.

Petersilka M, Gossmann UJ, Gross EKU. Excitation Energies from Time-Dependent Density-Functional Theory. *Physical Review Letters*, 1996, 76(8), 1212–1215.

Psciuk BT, Lord RL, Munk BH, Schlegel HB. Theoretical Determination of One-Electron Oxidation Potentials for Nucleic Acid Bases. *J. Chem. Theory Comput.* 2012, 8, 5107−5123.

Ratner S, Clarke HT. The Action of Formaldehyde upon Cysteine. *J. Am. Chem. Soc.* 1937, 59(1), 200–206.

Sahiba N, Sethiya A, Soni J, K. Agarwal DK, Agarwal S. Saturated Five-Membered Thiazolidines and Their Derivatives: From Synthesis to Biological Applications. *Top Curr Chem (Cham).* 2020; 378(2), 34.

Sirjean B, Fournet R, Glaude PA, Ruiz-Lopez MF. Extension of the composite CBS-QB3 method to singlet diradical calculations. *Chemical Physics Letters*, Elsevier, 2007, 435, 152 - -156.

Šakić D. Doktorski rad: Kvantno-kemijsko istraživanje reakcija pregrađivanja odabranih psihofarmaka. Farmaceutsko-biokemijski fakultet Sveučilišta u Zagrebu, 2015.

Tandarić T. Diplomski rad: Mehanizam reakcije kloriranja 5-fluorouracila. Farmaceutskobiokemijski fakultet Sveučilišta u Zagrebu, 2016.

Voityuk AA. xESE program, Girona, 2020. http://iqcc.udg.edu/~vybo/ESE/. Last access 13/08/2021.

Voityuk AA, Vyboishchikov SF. A simple COSMO-based method for calculation of hydration energies of neutral molecules. *Phys. Chem. Chem. Phys*., 2019, 21, 875–874.

Vyboishchikov SF, Voityuk AA. Fast and accurate calculation of hydration energies of molecules and ions. *Phys. Chem. Chem. Phys*. 2020, 22, 14591–14598.

Vyboishchikov SF, Voityuk AA. Fast non-iterative calculation of solvation energies for water and non-aqueous solvents. *J Comput Chem*. 2021, 1–11.

Wang B, Yan J, Li G,Zhang J, Zhang L, Li Z, Chen H (2020). Risk of penicillin fermentation dreg: Increase of antibiotic resistance genes after soil discharge. *Environmental Pollution,* 2020, 259, 113956.

7.   SUMMARY/SAŽETAK

Thiazolidine, a long-known and thoroughly tested molecule, is a structural part of many commonly used compounds. Among these are penicillin antibiotics, which can be found in the environment in increasing concentrations that already exhibit a number of harmful effects in both environmental and health aspects. In order to find a solution for this problem, in the laboratory where this thesis was made it was discovered that UV light only opens thiazolidine ring in thiazolidine and its derivatives. This discovery requires additional chemical description that cannot be obtained through experiments. Therefore, in this research computational methods were used to gather chemical descriptors for the mentioned process on thiazolidine and its three derivatives. For each derivative, species with open and closed thiazolidine rings were tested, as well as certain constants that describe the transition from one species to another.

All collected results in this work were calculated using Gibbs free energies of optimized structures at b3lyp/6-31G(d,p) and b3lyp/6-311++G(d,p) theoretical level. Solvation energies were obtained using the SMD method. Acidity constants were calculated using six different methods, of which method 5 proved to be the most accurate one. Transition state structure for thiazolidine ring-opening reaction was confirmed by IRC calculation, and the wavelengths of absorption maxima were confirmed by TD-DFT calculations.

The obtained values for acidity and chemical equilibrium constants give a basic insight into the behavior of tested species in water. Global reactivity indexes, accompanied by UV-Vis absorption maxima, show high reactivity for all examined compounds. For all molecules, the ratio of the constants values for the same reactions among the corresponding species is the same. The constants' absolute values for the molecules obtained differ depending on the substituents on the thiazolidine ring, as expected.

Tiazolidin, dobro poznata i temeljito ispitana molekula, strukturalni je dio mnogih, često korištenih spojeva. Među takvima su i penicilinski antibiotici, koje nalazimo u okolišu u sve većim koncentracijama koje već sada uzrokuju niz štetnih učinaka u ekološkom i zdravstvenom aspektu. S ciljem pronalaska rješenja za ovaj aktualni problem, u laboratoriju gdje je rađen ovaj rad otkriveno je da pod utjecajem UV svjetla dolazi do otvaranja tiazolidinskog prstena u tiazolidinu i njegovim derivatima. Ovo otkriće zahtijevalo je dodatno razumijevanje koje se eksperimentima za ovaj brzi proces ne može dobiti. U tu su svrhu u ovom radu korištene računalne metode te su dobiveni kemijski parametri koji opisuju spomenuti proces na tiazolidinu i trima njegovim derivatima. Za svaki su derivat ispitane specije s otvorenim i zatvorenim tiazolidinskim prstenom, te određene konstante koje opisuju prelazak jedne specije u drugu.

Svi prikupljeni rezultati ovog rada izračunati su pomoću slobodnih Gibbsovih energija optimiziranih struktura na b3lyp/6-31G(d,p) i b3lyp/6-311++G(d,p) teorijskoj razini. Solvatacijske energije dobivene su pomoću SMD metode. Konstante kiselosti izračunate su pomoću šest različitih metoda, od kojih se metoda 5 pokazala najtočnijom. IRC računom potvrđena je struktura prijelaznog stanja reakcije otvaranja tiazolidinskog prstena, a TD-DFT računima valne duljine apsorpcijskih maksimuma.

Dobivene vrijednosti konstanti kiselosti i kemijske ravnoteže daju osnovni uvid u ponašanje specija u vodi. Indeksi reaktivnosti, popraćeni UV-Vis apsorpcijskim maksimumima, pokazuju visoku reaktivnost svih ispitivanih spojeva. Za sve molekule, odnos vrijednosti pojedinih konstanti za iste reakcije među odgovarajućim specijama je isti. Apsolutna vrijednost dobivenih brojki razlikuje se ovisno o supstituentima na tiazolidinskom prstenu, kao što je i očekivano.

8.   APPENDIX

Table 8. pK_a values calculated at b3lyp/6-311++G(d,p)/SMD level for thiazolidine, 2-methyl-thiazolidine, 2-(4'-hydroxy)-phenyl-thiazolidine and N-methyl-thiazolidine using the methods described in Materials and methods (3.10.).

| | $AH \rightarrow A^- + H^+$ | | $AH + R^- \rightarrow A^- + RH$ | | $AH + H_2O \rightarrow A^- + H_3O^+$ | | |
	Method 1	Method 2	Method 3	Method 4	Method 5 SMD	xESE	Method 6
			Thiazolidine				
$pK_{a(1,2)}$	3.62	3.46	1.61	16.75	3.24	5.48	15.29
$pK_{a(3,2)}$	-4.46	-4.43	-6.28	8.86	-4.84	-1.41	7.21
$pK_{a(4,6)}$	6.32	6.23	4.38	29.52	5.93	7.51	17.99
$pK_{a(4,5)}$	14.59	14.90	13.04	28.19	14.21	25.08	26.26
			2-methyl-thiazolidine				
$pK_{a(1,2)}$	3.77	3.59	1.73	16.88	3.39	1.57	15.44
$pK_{a(3,2)}$	-2.33	-2.39	-4.24	10.90	-2.71	3.12	9.34
$pK_{a(4,6)}$	9.44	9.84	7.99	23.13	9.06	7.55	21.11
$pK_{a(4,5)}$	14.6	15.62	13.77	28.91	14.22	36.82	26.27
			2-(4'-hydroxy)-phenyl-thiazolidine				
$pK_{a(1,2)}$	-1.04	-0.96	-2.82	12.32	-1.42	1.57	10.63
$pK_{a(3,2)}$	4.55	4.51	2.65	17.80	4.16	3.12	16.22
$pK_{a(4,6)}$	11.86	12.20	10.35	25.49	11.48	7.55	23.53
$pK_{a(4,5)}$	26.93	27.62	25.76	40.90	26.54	36.82	38.60
			N-methyl-thiazolidine				
$pK_{a(1,2)}$	5.18	4.94	3.08	18.22	4.79	4.94	16.85
$pK_{a(3,2)}$	-1.09	-1.46	-3.32	11.82	-1.47	-2.47	10.58
$pK_{a(4,5)}$	14.42	15.05	13.20	28.34	14.04	23.65	26.09

Table 9. Chemical equilibrium constants (K_{eq}) for chemical reactions shown in Figures 9 and 10 calculated at b3lyp/6-311++G(d,p)/SMD level.

K_{eq}	Thiazolidine	2-methyl-thiazolidine	2-(4'-hydroxy)-phenyl-thiazolidine	N-methyl-thiazolidine
$K_{eq(1,3)}$	$1.29 \cdot 10^{-8}$	$1.06 \cdot 10^{-7}$	$29.81 \cdot 10^{4}$	$4.01 \cdot 10^{-7}$
$K_{eq(6,5)}$	$2.15 \cdot 10^{-9}$	$1.67 \cdot 10^{-6}$	$3.87 \cdot 10^{-16}$	-
$K_{eq(2,6)}$	$2.63 \cdot 10^{-9}$	$5.90 \cdot 10^{-6}$	$8.74 \cdot 10^{-9}$	-
$K_{eq(3,4)}$	119.00	$1.00 \cdot 10^{7}$	0.43	50.78
$K_{eq(2,5)*}$	-	-	-	$1.55 \cdot 10^{-15}$

*N-methyl-thiazolidine only

40

Table 10. HOMO-LUMO energy gap, chemical hardness (η), softness (S), chemical potential (μ), electronegativity (χ) and electrophilicity index (ω) calculated at b3lyp/6-311++G(d,p) /SMD level. All values are expressed in eV. Numbers from 1 to 6 correspond to the species in Figures 9 and 10.

	HOMO-LUMO	η	S	μ	χ	ω
Thiazolidine						
1	0.232	0.116	8.624	-0.130	0.130	0.073
2	0.217	0.109	9.199	-0.112	0.112	0.058
3	0.186	0.093	10.752	-0.176	0.176	0.167
4	0.166	0.083	12.065	-0.173	0.173	0.180
5	0.093	0.047	21.425	-0.129	0.129	0.179
6	0.217	0.109	9.210	-0.133	0.133	0.082
2-methyl-thiazolidine						
1	0.238	0.119	8.415	-0.134	0.134	0.075
2	0.218	0.109	9.172	-0.111	0.111	0.057
3	0.190	0.095	10.500	-0.168	0.168	0.148
4	0.182	0.091	10.990	-0.163	0.163	0.146
5	0.109	0.055	18.308	-0.120	0.120	0.133
6	0.231	0.115	8.667	-0.126	0.126	0.069
2-(4'-hydroxy)-phenyl-thiazolidine						
1	0.211	0.105	9.490	-0.134	0.134	0.085
2	0.196	0.098	10.198	-0.121	0.121	0.074
3	0.156	0.078	12.850	-0.171	0.171	0.187
4	0.156	0.078	12.807	-0.170	0.170	0.186
5	0.088	0.044	22.635	-0.132	0.132	0.197
6	0.182	0.091	10.998	-0.134	0.134	0.099
N-methyl-thiazolidine						
1	0.232	0.116	8.612	-0.130	0.130	0.073
2	0.217	0.109	9.201	-0.112	0.112	0.057
3	0.183	0.092	10.909	-0.171	0.171	0.160
4	0.173	0.087	11.538	-0.170	0.170	0.166
5	0.098	0.049	20.367	-0.127	0.127	0.163

Table 11. Excitation wavelength (λ) with corresponding oscillator strength (f) calculated at b3lyp/6-311++G(d,p)/SMD level.

Species	Thiazolidine		2-methyl-thiazolidine		2-(4'-hydroxy)-phenyl-thiazolidine		N-methyl-thiazolidine	
	λ\ nm	f	λ\ nm	f	λ\ nm	f	λ\ nm	f
1	196.43	0.0361	156.64	0.0235	239.31	0.1217	157.29	0.0218
	144.73	0.0343	149.82	0.0207	208.18	0.1059	146.06	0.0212
	140.81	0.0958	146.37	0.0606	206.43	0.1069	144.46	0.0464
2	203.99	0.0379	207.78	0.0243	226.22	0.0742	220.22	0.0296
	193.73	0.0282	190.27	0.0908	222.12	0.0571	216.25	0.0219
	175.55	0.1463	184.93	0.0222	219.07	0.0498	190.85	0.0376
3	193.01	0.0276	164.45	0.0454	250.25	0.0463	199.73	0.0363
	159.37	0.0626	163.73	0.0329	239.31	0.1811	179.49	0.0647
	142.49	0.1009	157.65	0.0261	204.69	0.1134	157.8	0.031
4	494.23	0.0201	360.54	0.0763	400.81	0.1188	365.58	0.0839
	189.32	0.0316	172.04	0.2514	302.37	0.4495	170.68	0.0857
	172.2	0.0373	167.77	0.0754	294.71	0.1047	168.66	0.0716
5	630.27	0.2076	674.51	0.2011	764.89	0.1634	691.15	0.1754
	278.32	0.0281	277.79	0.0314	420.82	0.0274	280.33	0.0297
	252.6	0.0364	273.93	0.0517	329.22	0.1295	272.56	0.0196
6	213.1	0.0178	212.82	0.0115	267.8	0.2584	-	-
	180.01	0.0259	182.45	0.0264	255.51	0.2244	-	-
	173.27	0.0129	180.28	0.0143	215.45	0.0906	-	-

Table 12. Optimized geometries for thiazolidine, 2-methyl-thiazolidine, 2-(4'-hydroxy)-phenyl-thiazolidine, N-methyl-thiazolidine (species 1 to 6) and transition state (TS) optimized structure for 2-(4'-hydroxy)-phenyl-thiazolidine reaction 2-6, calculated at b3lyp/6-31G(d,p)/SMD level.

THIAZOLIDINE

1

C	-0.12800100	1.34988800	-0.12433300
C	1.22365900	0.77904300	0.27299400
H	-0.42396900	2.14963600	0.55484600
H	-0.12155800	1.72512200	-1.14875500
S	-1.33958800	-0.05155100	-0.00411200
H	1.33838100	0.70351200	1.35460400
H	2.05999400	1.33061400	-0.15621200
N	1.25277800	-0.62906900	-0.26245600
C	-0.01201500	-1.31561700	0.15196200
H	1.32599100	-0.61085000	-1.28598400
H	-0.19439500	-2.16652800	-0.50174800
H	0.11158300	-1.64298500	1.18342800
H	2.06607000	-1.14010700	0.09905800

2

C	0.03022700	1.32921100	-0.11794900
C	-0.02353800	-1.32298800	0.14903600
C	-1.29429500	0.63814300	0.26077100
H	0.27490200	2.14586800	0.56467300
H	-0.00283600	1.71824900	-1.13880100
H	0.24031800	-2.17435700	-0.47761300
H	-0.04824400	-1.63105800	1.19557600
H	-2.15065100	1.18050000	-0.14678700
H	-1.39347400	0.61002000	1.35053100
S	1.31883700	0.01009000	-0.00854800
N	-1.28469900	-0.74066700	-0.24291000
H	-1.30287400	-0.69217800	-1.26158600

3

C	-0.11454800	1.34668200	-0.26015100
C	-0.34817800	-1.29680500	-0.25534900
C	-0.63517400	0.66426100	1.00126400
H	0.78810100	1.94328000	-0.13325400
H	-0.88048000	1.90922400	-0.79322000
H	0.48913500	-1.69977600	0.32731900
H	-0.82087500	-2.10486500	-0.81527100
H	-1.33603800	1.32527600	1.51429500
H	0.20055600	0.43328900	1.67561500
S	0.28358600	-0.09958500	-1.38034100
N	-1.32962000	-0.53352700	0.50930800
H	-1.65527600	-1.11369600	1.28092100
H	1.61120200	-0.220995-00	-1.12628600

4

C	0.75212000	1.00148800	-0.20026000
C	-1.95142300	-1.00777200	0.10248100
C	-0.64817300	1.02962500	0.41788600
H	1.34882700	1.77679400	0.28317100
H	0.70596800	1.23241700	-1.26744700
H	-1.65375300	-1.35984200	1.08496900
H	-2.58747900	-1.60801700	-0.53938400
H	-1.05139500	2.04220600	0.34167100
H	-0.63757600	0.72652300	1.46512900
S	1.62331700	-0.61293300	-0.07527900
N	-1.56838500	0.14254600	-0.30135100
H	-1.85315500	0.44639900	-1.23485400
H	1.81904200	-0.58743200	1.26002600

5

C	0.12303900	1.64419500	0.05545600
C	-0.45095200	-1.72143100	0.07172800
C	-1.02580600	0.65757200	0.30126000
H	0.21182600	1.81484600	-1.02500700
H	-0.34855300	-1.80764100	1.14917800
H	-1.97064600	1.07190900	-0.05406000
H	-1.11417500	0.40446600	1.35821700
N	-0.81255700	-0.60661700	-0.43727700
H	-0.88648600	-0.54732900	-1.45435400
H	1.05381300	1.16356400	0.38154400
S	-0.17007000	3.22157200	0.95639900
H	-0.25544800	-2.56770700	-0.57801400

6

C	-0.49445800	0.78313600	0.58390100
C	1.72157300	-1.04013700	0.28359300
C	0.76083600	1.06530500	-0.23725800
H	-1.05224700	1.71683800	0.67462200
H	-0.24995900	0.43279200	1.58954200
H	0.92672600	-1.29363400	0.99045800
H	2.51197700	-1.78276200	0.16477800
H	1.25749400	1.93300300	0.21428300
H	0.47410600	1.38729800	-1.24391100
S	-1.60248100	-0.45642700	-0.24441500
N	1.79177600	0.03707900	-0.39402900
H	-2.69854000	-0.20007300	0.49766300

2-METHYL-THIAZOLIDINE

1
```
C   -1.67021400 -0.35751700 0.26714200
C   -1.40313600 1.08476000 -0.16855800
H   -1.83812400 -0.42851500 1.34362900
H   -2.53002400 -0.77237100 -0.26005600
S   -0.16290900 -1.30057500 -0.18238900
H   -1.88949700 1.80799100 0.48491800
H   -1.70585800 1.25749000 -1.19952600
N    0.10116100 1.32666600 -0.10558300
C    0.84591800 0.10385100 0.41314900
H    0.44727500 1.54935300 -1.04466600
H    0.77248100 0.15910600 1.50086500
H    0.31686800 2.13045200 0.49371600
C    2.28854700 0.09416200 -0.04680600
H    2.80656000 0.98001600 0.33178900
H    2.79170300 -0.78837200 0.35523500
```

2
```
C   -1.68117800 -0.26504000 0.27382200
C    0.87381900 0.23516800 -0.39733100
C   -1.28117600 1.15236600 -0.18453600
H   -2.54334200 -0.64372500 -0.27996200
H   -1.91196300 -0.28477400 1.34207300
H    0.93081600 0.29861900 -1.48651200
H   -1.88819400 1.91244900 0.31315000
H   -1.43770500 1.24460400 -1.26398600
S   -0.20265000 -1.31573400 -0.05342700
N    0.13849700 1.37393400 0.10200200
H    0.25227400 1.39576000 1.11672200
C    2.26002800 0.09678600 0.20059300
H    2.76608700 -0.79046700 -0.18896300
H    2.86574400 0.97184300 -0.05813000
H    2.21023800 0.01421700 1.29114100
```

3
```
C    0.02214800 1.37124900 -0.16721300
C    0.06582900 -1.29611800 0.02520800
C   -1.23306100 0.65097800 0.32484600
H    0.45058300 2.09282500 0.52777200
H   -0.09628300 1.81157600 -1.15681900
H    0.17055800 -1.45536400 1.10728900
H   -2.12124300 1.20849100 0.02203000
H   -1.21484100 0.57438800 1.42043100
S    1.23645700 -0.02542300 -0.40643200
N   -1.19408300 -0.65381600 -0.34505000
H   -1.95892400 -1.25324800 -0.03809700
C    0.32344100 -2.59433200 -0.72262600
H    1.28986700 -3.02135000 -0.44318200
H   -0.45485200 -3.30975300 -0.44242900
H    0.29182600 -2.44440300 -1.80478600
H    1.92163700 0.06070200 0.76164500
```

4
```
C    1.51573000 0.79248500 -0.33726500
C   -1.69695000 -0.11059000 0.40651700
C    0.26676000 1.35020200 0.34600300
H    2.37696500 1.37230500 -0.00040800
H    1.44283500 0.90404700 -1.42219600
H   -1.41346800 -0.37223300 1.42356100
H    0.21415100 2.42687300 0.16526200
H    0.28241000 1.17356900 1.42218600
S    1.82802200 -0.99691100 -0.04147600
N   -0.96211700 0.75796200 -0.19337200
H   -1.20158800 1.00846600 -1.15473600
H    2.13130800 -0.89316600 1.26963300
C   -2.88289700 -0.73707800 -0.20073700
H   -2.74532100 -1.82472000 -0.18311700
H   -3.75315500 -0.52440000 0.43141600
H   -3.06353300 -0.39600300 -1.22148600
```

5
```
C    0.05969300 1.73425800 0.05493100
C   -0.29318100 -1.69806700 0.03634700
C   -0.98877500 0.65101800 0.32152300
H    0.09589800 1.92654400 -1.02531300
H   -0.19168700 -1.75298300 1.11855700
H   -1.97911100 0.99475600 0.01624800
H   -1.01727800 0.37702700 1.37684300
N   -0.70925600 -0.58300300 -0.44728100
H   -0.79632300 -0.50774800 -1.46219900
C    0.03905500 -2.87616900 -0.78547000
H    1.07826700 -3.16237000 -0.58454900
H   -0.58312800 -3.71837300 -0.46062400
H   -0.10042300 -2.69585000 -1.85299200
H    1.04140600 1.33582400 0.34020900
S   -0.33403300 3.27310200 0.98878300
```

6
```
C   -1.24646100 0.67073700 0.61094300
C    1.49776100 -0.17821500 0.22355200
C   -0.20238100 1.42430400 -0.21090500
H   -2.11145200 1.32494200 0.73395200
H   -0.87311700 0.40921800 1.60378000
H    0.85287200 -0.68254700 0.95255100
H   -0.04991900 2.39542000 0.27730800
H   -0.62282200 1.65753700 -1.19510300
S   -1.82397900 -0.87060100 -0.24970500
N    1.12673600 0.85126700 -0.43392400
H   -2.92185100 -1.06678200 0.50797500
C    2.85484700 -0.78445500 0.05557800
H    3.38662800 -0.78907600 1.01508200
H    2.76455500 -1.83234100 -0.25602400
H    3.44901600 -0.23985100 -0.68177400
```

2-(4'-HYDROXY)-PHENYL-THIAZOLIDINE

1

C	-3.57956600	0.08288100	-0.32548500
C	-3.21778800	-0.17613400	1.13349700
H	-3.88071600	-0.83247700	-0.83966700
H	-4.37780600	0.82226700	-0.40374400
S	-2.04823200	0.74639300	-1.08035100
H	-3.84091400	-0.94545500	1.58877000
H	-3.26737900	0.73725100	1.72327300
N	-1.77179200	-0.65066300	1.17701800
C	-1.08537300	-0.54428600	-0.20003900
H	-1.25065600	-0.09334200	1.86033400
H	-1.27430400	-1.50706200	-0.67586300
H	-1.72014600	-1.62727700	1.48425000
C	0.38933600	-0.28605300	-0.09834800
C	1.28771600	-1.26661600	-0.53801600
C	0.89856200	0.91435400	0.42452700
C	2.66293100	-1.06285800	-0.46056800
H	0.90825400	-2.19860600	-0.94668300
C	2.26872300	1.12549600	0.51364300
H	0.22048700	1.69093500	0.76680400
C	3.15564800	0.13519800	0.06889800
H	3.35487400	-1.82581600	-0.80572900
H	2.66546700	2.05013100	0.91935200
O	4.49445900	0.39619900	0.17822600
H	5.00028800	-0.35967900	-0.15906800

2

C	-3.48889000	-0.56957700	0.19706100
C	-1.11147000	0.60741000	-0.27459500
C	-3.16827700	0.78864000	0.87029300
H	-4.45101800	-0.54740000	-0.32077400
H	-3.50718700	-1.38163200	0.93017300
H	-1.27079200	1.43491000	-0.97087800
H	-3.63762800	0.87509600	1.85500100
H	-3.55187300	1.60163300	0.24323500
S	-2.13042200	-0.85320700	-1.00870800
N	-1.72378900	0.94519700	0.99118400
H	-1.36225900	0.32538200	1.71390600
C	0.36282200	0.30929700	-0.16758300
C	1.29743300	1.23303800	-0.64460800
C	0.83910300	-0.85875000	0.44718800
C	2.66735600	1.01035700	-0.50969200
H	0.95287100	2.14459500	-1.12538700
C	2.20095100	-1.09196400	0.59507700
H	0.12932200	-1.60614800	0.78965500
C	3.12308400	-0.15391700	0.11510500
H	3.37917100	1.74016400	-0.88957500
H	2.57055100	-1.99690600	1.06549300
O	4.44933400	-0.43537800	0.28005500
H	4.97477800	0.28106600	-0.09973000

3

C	-0.02399000	1.30950000	-0.24650900
C	0.12476300	-1.32040400	0.14178500
C	-1.22468000	0.60324700	0.40842200
H	0.36746800	2.17457300	0.29111000
H	-0.20268700	1.56241300	-1.29270300
H	0.29775600	-1.51529200	1.20230300
H	-2.15326600	1.09112400	0.10962900

4

C	-3.77347800	-0.52763700	-0.30634500
C	-0.56595500	-0.19312400	0.83882400
C	-2.87087800	-1.01937900	0.82638000
H	-4.81322600	-0.66308500	-0.00214800
H	-3.61146400	-1.11939300	-1.21104500
H	-0.91429000	0.54953400	1.55232000
H	-3.16941500	-2.03764500	1.09099800
H	-2.96642700	-0.39093000	1.71312400
S	-3.50883500	1.22228800	-0.81176700
N	-1.45870900	-1.05794400	0.44635200
H	-1.20167700	-1.76781300	-0.23664900
H	-3.95780900	1.78975400	0.32762700
C	0.80616000	-0.14113900	0.43973000
C	1.59994400	0.88631500	0.99883400
C	1.40238100	-1.04443000	-0.47494900
C	2.93448300	1.01924100	0.66139400
H	1.15014200	1.58009100	1.70234100
C	2.73277500	-0.91832500	-0.81495700
H	0.82480000	-1.84832300	-0.92029300
C	3.50580800	0.11726400	-0.25112900
H	3.54291000	1.80974800	1.08983400
H	3.20079100	-1.60243400	-1.51401100
O	4.80074200	0.19188300	-0.63046500
H	5.23461000	0.94171300	-0.19126600

5

C	-1.14850900	-0.02341400	0.44232800
C	2.00721700	-0.27816500	-0.42057400
C	-0.11776600	0.86722700	-0.25949200
H	-1.06680600	0.12666500	1.52537100
H	1.62437700	-0.72528100	-1.33080400
H	-0.31012600	1.91964400	-0.05826800
H	-0.12329100	0.70311300	-1.33689000
N	1.27568500	0.56670500	0.21743400
H	-0.87881300	-1.06824500	0.24061800
S	-2.84278200	0.36219100	-0.15799700
H	2.99545300	-0.52913500	-0.05314900
C	1.69771800	1.10631800	1.48892100
C	1.55705000	2.47257200	1.74868400
C	2.25398200	0.25219900	2.44841400
C	1.98986800	2.98761900	2.96519700
H	1.14308900	3.14099200	1.00246400
C	2.68087000	0.76637100	3.66538100
H	2.32680600	-0.81252900	2.25301400
C	2.55278500	2.13725100	3.92620700
H	1.89875000	4.04971100	3.17154200
H	3.10093500	0.11580600	4.42459800
O	2.98709000	2.58979200	5.13794200
H	2.84006200	3.54677900	5.19837700

6

C	-3.58289700	0.11734900	0.66427600
C	-0.70089500	0.27286700	0.38962300
C	-2.80246000	1.38079900	0.30461100
H	-4.60857100	0.41208900	0.89368600
H	-3.16812700	-0.38384600	1.54178700
H	-1.17127600	-0.61149100	0.83396400
H	-2.95934100	2.09763100	1.12189600

H	-1.13257700 0.64945700 1.49668400
S	1.26334100 -0.01664700 -0.27265000
N	-1.21927200 -0.79226400 -0.02358200
C	0.39685600 -2.58261800 -0.64395300
C	0.72509500 -3.76026600 0.03615600
C	0.31397400 -2.60900900 -2.04474100
C	0.95921100 -4.94485800 -0.65852800
H	0.79627200 -3.75426700 1.11989700
C	0.54615800 -3.78421500 -2.74917500
H	0.06614200 -1.70801100 -2.60158000
C	0.87081000 -4.95730100 -2.05456200
H	1.21181700 -5.85705500 -0.12520100
H	0.48379400 -3.80696600 -3.83197900
O	1.09495600 -6.08672500 -2.79506300
H	1.32058200 -6.81896700 -2.20057100
H	-1.48920800 -0.84603100 -1.00621700
H	1.81885400 0.21198100 0.94444000

H	-3.26029400 1.84367900 -0.57668800
S	-3.64204600 -1.08176900 -0.75274600
N	-1.36255100 1.31892200 0.06268700
H	-4.62703400 -1.85651900 -0.25523100
C	0.75216600 0.14860300 0.20758100
C	1.38585400 -1.04102800 0.60113500
C	1.54228500 1.17335300 -0.34728600
C	2.75938100 -1.21296300 0.45239400
H	0.79209500 -1.84352800 1.03087300
C	2.91159200 1.01545300 -0.50220900
H	1.07008500 2.09907000 -0.65759600
C	3.52584700 -0.18129600 -0.10120100
H	3.24109700 -2.13708500 0.76015200
H	3.52192300 1.80453400 -0.92981700
O	4.88105500 -0.28041300 -0.27666100
H	5.18635000 -1.14419300 0.04183000

TS₂₋₆

C	-0.09536600 1.33608400 -0.08527100
C	0.07836100 -1.28863000 0.12914800
C	-1.33569000 0.56810300 0.41188600
H	0.21969300 2.11314800 0.61445200
H	-0.26139400 1.78677700 -1.06658100
H	0.16134200 -1.51768900 1.19599500
H	-2.25815500 1.05760400 0.09133000
H	-1.32903800 0.53719300 1.50601200
S	1.20915300 0.03574300 -0.23861000
N	-1.29666500 -0.80964400 -0.09237800
C	0.38643100 -2.56074300 -0.63612100
C	0.65984500 -3.74546400 0.05598600
C	0.38489300 -2.59690900 -2.03934600
C	0.92378000 -4.93672200 -0.62123000
H	0.66776800 -3.74083800 1.14266700
C	0.63683800 -3.77808700 -2.72996900
H	0.18923600 -1.68834100 -2.60222100
C	0.91098400 -4.95308400 -2.01849600
H	1.13909100 -5.84961100 -0.07214500
H	0.63172000 -3.80316300 -3.81509600
O	1.16400100 -6.09200800 -2.74580800
H	1.34781600 -6.82193600 -2.13478200
H	-1.44315300 -0.76956000 -1.10268400

N-METHYL-THIAZOLIDINE

1
C -1.10312600 1.21722400 -0.09217100
C 0.38007900 1.24537800 0.24105700
H -1.67218300 1.80588100 0.62763500
H -1.29788200 1.58695400 -1.09981700
S -1.62257300 -0.56390400 0.00150800
H 0.56225300 1.21967400 1.31666300
H 0.89688000 2.09507700 -0.20584600
N 0.97444800 -0.02159900 -0.32255700
C 0.11053500 -1.15538200 0.14264400
H 0.90438600 0.02980200 -1.34589500
H 0.38004100 -1.36961000 1.17697600
H 0.28527100 -2.02653600 -0.48752700
C 2.41823000 -0.20946800 0.02955500
H 2.76354500 -1.14055100 -0.41836000
H 2.97756300 0.63501500 -0.37148000
H 2.50585500 -0.24855200 1.11491100

2
C 0.74345700 1.24320200 -0.29776400
C -0.06034900 -1.10135900 0.67833800
C -0.50518600 1.17532300 0.61247100
H 1.46834300 1.96728900 0.07911000
H 0.48440100 1.50729200 -1.32542800
H -0.32292200 -2.08957500 0.30089100
H 0.22760900 -1.17123400 1.72828400
H -1.22672400 1.95366500 0.35272500
H -0.19683900 1.32664800 1.65157900
S 1.46497800 -0.45484000 -0.26545800
N -1.12908600 -0.15081600 0.50262800
C -1.82667500 -0.32427700 -0.78101500
H -2.29956200 -1.30915300 -0.80526900
H -2.61040100 0.43211100 -0.86831700
H -1.16743000 -0.24123200 -1.65682200

3
C 0.10378200 1.36020000 0.04402400
C 0.02803500 -1.28832900 0.47408000
C -1.22880300 0.67029200 0.35532900
H 0.38320600 2.12036400 0.77202200
H 0.16753500 1.75893700 -0.96775000
H -0.00315100 -1.35776000 1.57121900
H 0.33879000 -2.23675000 0.03398300
H -2.04192300 1.19846100 -0.14688000
H -1.41241800 0.69332000 1.44056100
S 1.38150700 -0.00256000 0.15008900
N -1.13268600 -0.70472600 -0.15203000
C -2.32974500 -1.50337800 0.15689700
H -3.19166500 -1.05146500 -0.33811200
H -2.20118700 -2.51748300 -0.22765100
H -2.53116800 -1.55665900 1.23725300
H 1.51557600 -0.23289300 -1.17984300

4
C -0.91916000 -1.05115700 0.09501400
C 1.23655900 1.44319600 0.34039600
C 0.31985200 -0.69906600 0.92560900
H -1.51516000 -1.75483000 0.67886500
H -0.64187000 -1.54685500 -0.83759400
H 0.57308600 1.88343900 1.07612900
H 1.89565100 2.06877400 -0.25216800
H 0.85494100 -1.61731300 1.17830000
H 0.04229300 -0.18637800 1.84701500
S -1.96950100 0.37535600 -0.39580100
N 1.26461700 0.17113700 0.19096800
H -2.43912300 0.66466100 0.83630500
C 2.15887900 -0.48610400 -0.77886200
H 1.55480500 -1.04005600 -1.49948400
H 2.75810300 0.26616200 -1.28857800
H 2.80018700 -1.18248400 -0.23569400

5
C -1.04024300 -0.42383200 0.41298700
C 2.04371400 0.07358300 -0.55971200
C -0.24094000 0.76019700 -0.14753600
H -0.90685400 -0.46376600 1.50057900
H 1.70570200 -0.31228300 -1.51564900
H -0.60351600 1.70500800 0.25806900
H -0.30588700 0.78630700 -1.23553200
N 1.20939400 0.67174800 0.20458300
H -0.60499000 -1.34334500 0.00105000
S -2.81916800 -0.26687200 -0.02695000
H 3.07758900 -0.03879500 -0.25149700
C 1.60467100 1.21010900 1.51557700
H 0.99721000 0.73296000 2.28634300
H 2.66115900 1.01317400 1.68946100
H 1.41006900 2.28417800 1.52015800

Table 13. Gibbs free energies (G) for thiazolidine, 2-methyl-thiazolidine, 2-(4'-hydroxy)-phenyl-thiazolidine, N-methyl-thiazolidine (species 1 to 6) calculated at b3lyp/6-31G(d,p)/SMD and b3lyp/6-311++G(d,p)/SMD level.

	G/Hartree					
Basis set	**1**	**2**	**3**	**4**	**5**	**6**
Thiazolidine						
6-31G(d,p)	-571.855496	-571.410387	-571.836351	-571.841115	-571.366778	-571.389263
6-311++G(d,p)	-571.919014	-571.48076	-571.901866	-571.906386	-571.443265	-571.462108
2-methyl-thiazolidine						
6-31G(d,p)	-611.150131	-610.704571	-611.143364	-611.150536	-610.675236	-610.691052
6-311++G(d,p)	-611.221829	-610.783298	-611.208838	-611.22406	-610.759372	-610.77193
2-(4'-hydroxy)-phenyl-thiazolidine						
6-31G(d,p)	-878.066279	-877.622226	-878.069882	-878.077129	-877.568276	-877.614829
6-311++G(d,p)	-878.199614	-877.770983	-878.211515	-878.210721	-877.719958	-877.753464
N-methyl-thiazolidine						
6-31G(d,p)	-611.13884	-610.691379	-611.123165	-611.126602	-610.652675	-
6-311++G(d,p)	-611,209664	-610,768207	-611,195758	-611,199466	-610,736009	-

OTVARANJE I DEPROTONIRANJE TIAZOLIDINSKOG PRSTENA. RAČUNALNA DFT STUDIJA.

Tea Kuvek

SAŽETAK

Tiazolidin, dobro poznata i temeljito ispitana molekula, strukturalni je dio mnogih, često korištenih spojeva. Među takvima su i penicilinski antibiotici, koje nalazimo u okolišu u sve većim koncentracijama koje već sada uzrokuju niz štetnih učinaka u ekološkom i zdravstvenom aspektu. S ciljem pronalaska rješenja za ovaj aktualni problem, u laboratoriju gdje je izrađen ovaj rad otkriveno je da pod utjecajem UV svjetla dolazi do otvaranja tiazolidinskog prstena u tiazolidinu i njegovim derivatima. Ovo otkriće zahtijeva dodatno razumijevanje koje se eksperimentima za ovaj brzi proces ne može dobiti. U tu su svrhu u ovom radu korištene računalne metode te su dobiveni kemijski parametri koji opisuju spomenuti proces na tiazolidinu i trima njegovim derivatima. Za svaki su derivat ispitane specije s otvorenim i zatvorenim tiazolidinskim prstenom, te određene konstante koje opisuju prelazak jedne specije u drugu.

Svi prikupljeni rezultati ovog rada izračunati su pomoću slobodnih Gibbsovih energija optimiziranih struktura na b3lyp/6-31G(d,p) i b3lyp/6-311++G(d,p) teorijskoj razini. Solvatacijske energije dobivene su pomoću SMD metode. Konstante kiselosti izračunate su pomoću šest različitih metoda, od kojih se metoda 5 pokazala najtočnijom. IRC računom potvrđena je struktura prijelaznog stanja reakcije otvaranja tiazolidinskog prstena, a TD-DFT računima valne duljine apsorpcijskih maksimuma.

Dobivene vrijednosti konstanti kiselosti i kemijske ravnoteže daju osnovni uvid u ponašanje specija u vodi. Indeksi reaktivnosti, popraćeni UV-Vis apsorpcijskim maksimumima, pokazuju visoku reaktivnost svih ispitivanih spojeva. Za sve molekule, odnos vrijednosti pojedinih konstanti za iste reakcije među odgovarajućim specijama je isti. Apsolutna vrijednost dobivenih brojki razlikuje se ovisno o supstituentima na tiazolidinskom prstenu, kao što je i očekivano.

Rad je pohranjen u Središnjoj knjižnici Sveučilišta u Zagrebu Farmaceutsko-biokemijskog fakulteta.

Basic documentation card

THIAZOLIDINE RING-OPENING AND DEPROTONATION. COMPUTATIONAL DFT STUDY.

Tea Kuvek

SUMMARY

Thiazolidine, a long-known and thoroughly tested molecule, is a structural part of many commonly used compounds. Among these are penicillin antibiotics, which can be found in the environment in increasing concentrations that already exhibit a number of harmful effects in both environmental and health aspects. In order to find a solution for this problem, in the laboratory where this thesis was made it was discovered that UV light only opens thiazolidine ring in thiazolidine and its derivatives. This discovery requires additional chemical description that cannot be obtained through experiments. Therefore, in this research computational methods were used to gather chemical descriptors for the mentioned process on thiazolidine and its three derivatives. For each derivative, species with open and closed thiazolidine rings were tested, as well as certain constants that describe the transition from one species to another.

All collected results in this work were calculated using Gibbs free energies of optimized structures at b3lyp/6-31G(d,p) and b3lyp/6-311++G(d,p) theoretical level. Solvation energies were obtained using the SMD method. Acidity constants were calculated using six different methods, of which method 5 proved to be the most accurate one. Transition state structure for thiazolidine ring-opening reaction was confirmed by IRC calculation, and the wavelengths of absorption maxima were confirmed by TD-DFT calculations.

The obtained values for acidity and chemical equilibrium constants give a basic insight into the behavior of tested species in water. Global reactivity indexes, accompanied by UV-Vis absorption maxima, show high reactivity for all examined compounds. For all molecules, the ratio of the constants values for the same reactions among the corresponding species is the same. The constants' absolute values for the molecules obtained differ depending on the substituents on the thiazolidine ring, as expected.